CALIFORNIA ENERGY COMMISSION

ENERGY RESEARCH AND DEVELOPMENT DIVISION

FINAL PROJECT REPORT

Seabirds in 3D: A Framework to Evaluate Collision Vulnerability With Future Offshore Wind Developments

July 2025 | CEC-500-2025-037

PREPARED BY:

Eli Wallach Charles Chamberlin Arne Jacobson
The Schatz Energy Research Center at Cal Poly Humboldt

Stephanie R. Schneider Sophie B. Bernstein Sadie Trush
David G. Ainley Scott B. Terrill Sharon H. Kramer
H. T. Harvey & Associates
Primary Authors

David Stoms, Ph.D.
Project Manager
California Energy Commission

Agreement Number: EPC-19-011

Alex Horangic
Branch Manager
SUSTAINABILITY AND RESILIENCE BRANCH

Jonah Steinbuck, Ph.D.
Director
ENERGY RESEARCH AND DEVELOPMENT DIVISION

Drew Bohan
Executive Director

ACKNOWLEDGEMENTS

Collaboration and funding for this study were provided by the California Energy Commission under grant agreement number EPC-19-011. This research would not have been possible without the valuable contributions of our project partners Glenn Ford and Janet Casey of R. G. Ford Consulting Company, Jarrod Santora of the National Oceanic and Atmospheric Administration Southwest Fisheries Science Center, Lisa Ballance of Oregon State University, and Jerome Qiriazi of the Humboldt Transit Authority. Ryan Terrill (Klamath Bird Observatory) provided technical guidance. The members of the project's Technical Advisory Committee provided valuable input: David Pereksta (Bureau of Ocean Energy Management), Chris Potter (California Department of Fish and Wildlife), Garry George (National Audubon Society), Dan Barton (Cal Poly Humboldt), Kaus Raghukumar (Integral Consulting), Mike Optis (National Renewable Energy Lab), Yi-Hui Wang (Ocean Protection Council), Mark Severy (Pacific Northwest National Laboratory), Tyler Studds (Ocean Winds), and Brita Woeck (Ørsted).

PREFACE

The California Energy Commission's (CEC) Energy Research and Development Division supports energy research and development programs to spur innovation in energy efficiency, renewable energy and advanced clean generation, energy-related environmental protection, energy transmission, and distribution and transportation.

In 2012, the Electric Program Investment Charge (EPIC) was established by the California Public Utilities Commission to fund public investments in research to create and advance new energy solutions, foster regional innovation, and bring ideas from the lab to the marketplace. The EPIC Program is funded by California utility customers under the auspices of the California Public Utilities Commission. The CEC and the state's three largest investor-owned utilities — Pacific Gas and Electric Company, San Diego Gas and Electric Company, and Southern California Edison Company — were selected to administer the EPIC funds and advance novel technologies, tools, and strategies that provide benefits to their electric ratepayers.

The CEC is committed to ensuring public participation in its research and development programs that promote greater reliability, lower costs, and increase safety for the California electric ratepayer and include:

- Providing societal benefits.
- Reducing greenhouse gas emissions in the electricity sector at the lowest possible cost.
- Supporting California's loading order to meet energy needs, first with energy efficiency and demand response, next with renewable energy (distributed generation and utility scale), and finally with a clean, conventional electricity supply.
- Supporting low-emission vehicles and transportation.
- Providing economic development.
- Using ratepayer funds efficiently.

Seabirds in 3D: A Framework to Evaluate Collision Vulnerability With Future Offshore Wind Developments is the final report for EPC-19-011 conducted by The Schatz Energy Research Center at Cal Poly Humboldt and H.T. Harvey & Associates. The information from this project contributes to the Energy Research and Development Division's EPIC Program.

For more information about the Energy Research and Development Division, please visit the CEC's research website (www.energy.ca.gov/research/) or contact the Energy Research and Development Division at ERDD@energy.ca.gov.

ABSTRACT

California aims to decarbonize electricity delivered to customers in the state, with a goal ensuring that 100 percent of electricity sales are from renewable sources and zero-carbon resources by 2045. Offshore wind is expected to play an important role in reaching this goal, due to the strong and reliable winds offshore California. Realizing the potential of offshore wind while minimizing impacts to biodiversity is also a priority for the state and many stakeholders. This study evaluates the potential tradeoffs between the collision vulnerability of 44 types of seabirds and offshore wind power-generation along California's coast. Using a multi-objective framework, the team assessed anticipated energy production and seabird densities at heights where seabirds are vulnerable to colliding with rotating turbine blades, highlighting regions that minimize seabird exposure while ensuring viable power generation. Long-term datasets suggest only about 8 percent of the seabird community is likely to be present at heights exceeding 10 meters above the sea surface, a height that serves as a conservative proxy for rotor swept heights. Furthermore, seabird populations are most dense nearshore and to the south, while the best wind resources are generally offshore and to the north. These findings can guide offshore wind site selection to ensure that California's renewable energy development considers seabird populations, focusing on those that are most likely to be exposed. Actual collisions are expected at a much lower rate than exposure because of species-specific behavior that could not be accounted for in this study.

Keywords: California Current System, collision vulnerability assessment, decision-making, offshore wind energy, seabirds, site selection, turbine, tradeoff analysis

Please use the following citation for this report:

Wallach, Eli, Charles Chamberlin, Arne Jacobson, Stephanie R. Schneider, Sophie B. Bernstein, Sadie Trush, David G. Ainley, Scott B. Terrill, and Sharon H. Kramer. 2025. *Seabirds in 3D: A Framework to Evaluate Collision Vulnerability With Future Offshore Wind Developments*. California Energy Commission. Publication Number: CEC-500-2025-037.

TABLE OF CONTENTS

LIST OF FIGURES

LIST OF TABLES

Executive Summary

Background

California is committed to having 100 percent renewable and zero-carbon electricity by 2045, as mandated by Senate Bill 100 (De Leon, Chapter 312, Statutes of 2018). Meeting this goal will require a diverse mix of energy sources, including offshore wind (OSW). OSW is a promising contributor to the state's electricity sources because of the strong, persistent winds associated with California's coastal and outer continental shelf waters. Recognizing this potential, California hopes to achieve 2 to 5 gigawatts of OSW capacity by 2030, increasing to 25 gigawatts by 2045.

Planning and installing OSW facilities requires addressing biological impacts to secure the necessary permits ahead of surveying, construction, and operation. Unlike existing OSW projects in relatively shallow Atlantic waters (less than 60 meters depth), areas being considered off California are much deeper (430 meters to 1,300 meters depth). These deep-water OSW facilities will host different seabirds, many whose flight behaviors are different than those of shallow water species.

There are decades of surveys from a two-dimensional (2D) perspective that address the densities of birds expected in an area, but they do not provide the bird presence and densities at the height at which these seabirds fly relative to the heights of wind turbines. This project developed a three-dimensional (3D) assessment of seabird density to support evaluating tradeoffs between seabird collision vulnerability and power generation focusing on California. These predictions highlight areas where OSW facilities could be sited to minimize seabird collisions while compromising little, if any, power generation potential. Insights from this framework can support critical decisions related to the location of future OSW facilities and can be adapted to address similar uncertainties and support OSW planning needs elsewhere.

Project Purpose and Approach

The project's primary goal was to improve understanding of potential seabird and wind facility interactions in waters off California to support decision-making for project siting, wind facility design, and environmental permitting. Specifically, the project team, led by the Schatz Energy Research Center at Cal Poly Humboldt, evaluated tradeoffs between seabird collision vulnerability and power generation potential within central and northern sections offshore where OSW planning is underway, in waters between Point Conception, California and Newport, Oregon. This project developed a framework to explore the tradeoff of two key factors:

1. Seabird densities expected at altitudes overlapping rotor-swept zones, using a 3D Seabird Collision Vulnerability Framework (3D Seabird Framework).
2. The average annual energy production expected under scenarios with different turbine numbers and sizes using an OSW Power Generation Model.

3D Seabird Framework: Extensive seabird and wind datasets were used to predict seabird densities in 3D, explicitly considering flight heights to evaluate collision vulnerability. The species most vulnerable to collision are those that are abundant and fly at heights overlapping rotor-swept zones (or, for this assessment, a more conservative 10 meters above sea level). Flight height is influenced by the interaction of wind speed with seabird size, shape, and flight style. Specifically, this 3D framework was used to predict the 2D and 3D densities for the 44 most frequently observed seabird species in the study area.

OSW Power Generation Model: Using the same wind dataset supporting the 3D Seabird Framework, average annual wind power production was estimated across the region and at eight key locations, including wind energy lease sites and several proposed and hypothetical areas of interest. At each location, the outcome of alternative turbine scenarios was then simulated with two turbine-capacity ratings (12 and 15 megawatts) and various facility build-out levels (single-turbine, 600 megawatts, and full buildout, as well as specific plans proposed by developers in cases where they were available). Power estimates were adjusted for a variety of factors that are normally expected to reduce generation from the maximum potential, such as efficiency losses and maintenance downtime.

Multi-objective Optimization Framework: The outcomes of the 3D Seabird Framework and the OSW Power Generation Model were combined using a common engineering approach that is well suited for examining tradeoffs between potentially competing objectives.

Key Results

The project provides critical insights into the tradeoffs between seabird exposure to rotor-swept zones and power generation potential, thus allowing seabird vulnerability to be considered when assessing options for siting future OSW facilities.

Seabird Community Predictions: Within the study area, seabirds were generally predicted to be most abundant close to shore, toward the southern end of the study area, and less than 10 meters above the sea surface. Only 8 percent of the seabird community was predicted to be above 10 meters, with 80 percent of these being either sooty shearwater — one of the most abundant dynamically soaring seabirds off California — or one of the nine species of gulls. Unfortunately, data were insufficient to model some less abundant species, several of which are federally threatened or endangered species (such as Hawaiian petrel and short-tailed albatross) at this time.

Power Generation Potential: In general, wind resources to support power generation were predicted to be best farther offshore and to the northern end of the study area and, specifically, off Cape Mendocino and northward into Southern Oregon. Otherwise, capacity factors in many locations were relatively large, ranging between 8 percent and 58 percent, and averaging 47 percent based on a single 12-megawatt turbine simulation at each location.

Optimization Analysis: Seabird collision vulnerability did not conflict appreciably with power generation, as seabirds were predicted to be most concentrated in areas that were spatially distinct from areas with the greatest potential to generate electricity from wind energy.

When considering all 44 seabird species included in the Optimization Framework, areas of Northern California at Cape Mendocino and Crescent City were found to have the greatest power generation and relatively low densities of seabirds above 10 meters. The Humboldt Wind Energy Area was similar, with slightly less power generation expected relative to the Cape Mendocino and Crescent City areas and similar seabird collision vulnerability. Areas in Central California and those closer to shore tended to generate less power and have greater collision vulnerability than those in Northern California.

Finding the optimal sites to support OSW energy facilities requires more than only knowledge of seabirds and electricity generation potential. Many technical, environmental, social, and financial factors must also be considered when making these consequential siting decisions. The possibility for seabird collisions with turbines has been one of many high-profile concerns held by stakeholders. This study has added important information in assessing the spatial variation of vulnerability of California seabirds as OSW planning moves forward.

These findings can be used immediately by energy agencies, regulators, developers, and other OSW stakeholders in making informed decisions that balance ecological considerations with renewable energy goals.

Knowledge Transfer and Next Steps

To disseminate results, the project team delivered the following:

- A public webinar hosted by the Schatz Energy Research Center on September 24, 2024: *Seabirds in 3D: A framework to evaluate collision vulnerability with future offshore wind developments.*
- Presentations at scientific meetings: Ocean Sciences Meeting, New Orleans, February 22, 2024; and Pacific Seabird Group Annual Meeting, Seattle, February 21–23, 2024: *Two novel approaches generate insight into seabird interactions with planned floating offshore wind facilities along the U.S. West Coast.*
- All interim reports: available by request from the California Energy Commission. Key interim reports are also available publicly at the Schatz Energy Research Center website (https://schatzcenter.org/wind/) and spatial predictions of seabird densities are available by request at https://zenodo.org/records/11620539.

Potential next steps to advance the scientific research on this topic include:

- Expanding species in the framework to those initially observed in less than 100 square kilometers.
- Including more recent seabird observations.
- Refining the framework for different OSW facility configurations.
- Conducting avoidance and collision risk modeling once wind turbines are in place.
- Enhancing seabird community predictions presented here for OSW planning by:
    - Expanding the Optimization Framework across a broader geographic range.
    - Validating the accuracy and reliability of 3D Seabird Framework predictions using emerging multi-sensor tracking technologies (such as the ThermalTracker-3D).

Potential applications of findings from this work are:

- Use of the spatial prediction files for the 44 seabird taxa that are available online to support various downstream and regional assessments.
- Inclusion in an expanded optimization analysis that incorporates important economic and socio-economic considerations in siting wind power facilities.

CHAPTER 1: Introduction

California is committed to having 100 percent renewable and zero-carbon electricity by 2045, as mandated by the Clean Energy Act of 2018 (Senate Bill 100, De Leon, Chapter 312, Statutes of 2018). Meeting this goal will require a diverse mix of energy sources, including offshore wind (OSW). OSW is promising due to the strong, predictable winds along California's coastal and outer continental shelf (OCS) regions (Rose et al. 2022). California aims to harness this potential by achieving 2 gigawatts to 5 gigawatts (GW) of OSW capacity by 2030 and scaling up to 25 GW by 2045 (Flint et al. 2022). Additionally, the Bureau of Ocean Energy Management (BOEM) has issued five lease areas in the deep (greater than 500 meters [m]) OCS waters off California for commercial wind development.

Installing OSW facilities off the U.S. West Coast presents several challenges related to permitting, construction, and operational planning. Unlike the relatively shallow waters of OSW projects along the U.S. East Coast and Europe, the deeper waters off the West Coast support a different assemblage of seabirds, a number of whose flight behaviors are different than those of nearshore species. These deeper waters require floating platforms anchored to the seafloor instead of the more conventional fixed platforms used in most OSW facilities. Moreover, the size of the turbines expected to be installed on the West Coast are larger than nearly all of those that have been installed elsewhere to date. As such, it may be misleading to generalize findings related to seabird-turbine interactions derived from studies at Atlantic and European OSW facilities with the interactions that may occur in the deeper waters off the West Coast.

Many seabird species with an affinity for these deeper, often offshore, waters (such as albatrosses, petrels, and shearwaters) fly using a specialized technique termed 'dynamic soaring.' This flight style involves harnessing winds to repeatedly ascend to great heights and then make forward progress by gliding downwards, conserving energy while traversing the Pacific Ocean (Pennycuick 1987a, b; Ainley et al. 2015). Flying in such an undulating fashion, while also achieving greater heights above the sea surface as wind speeds increase, likely makes dynamic soaring seabirds more vulnerable to collision with offshore wind turbines. This is due to an increased propensity to move about at the heights necessary to be struck by spinning blades comprising the wind-energy-turbine rotor-swept zone (RSZ), the primary potential hazard for birds encountering wind facilities (Masden and Cook 2016).

This assessment emphasizes the need to understand the spatial distribution and flight altitudes of seabirds to evaluate their collision vulnerability with OSW turbines. By estimating the density of seabirds flying at RSZ altitudes, the approach presented here generates this metric as a proxy for collision vulnerability, recognizing that vulnerability is distinct from collision rates. The analogy of a pedestrian crossing the street highlights this distinction: while crossing the street makes one vulnerable to being hit by a vehicle, most people who cross the street are not hit (that is, the rate of collision is only a fraction of the number of street crossings where the pedestrian may be vulnerable) due to avoidance behaviors, situational factors, and other dynamics. Similarly, seabird collisions with turbines are expected to be much lower than the densities exposed to the risk of collision, due to their propensity to actively avoid turbines at multiple spatial scales. For example, seabird studies using modern surveillance technologies in the Atlantic Ocean consistently show collision avoidance rates in excess of 99 percent (Williams et al. 2024, Cook et al. 2018, Skov et al. 2018, Tjørnløv et al. 2023). This study focuses on vulnerability (exposure) to collision, which is clearly distinct from expected or risk-modelled rates of collision.

Developing a predictive framework for seabird composition and density at RSZ-height off the West Coast is timely, given interest in developing OSW along the West Coast. Therefore, this project developed a three-dimensional (3D) assessment of seabird density to support evaluating tradeoffs between seabird collision vulnerability and power generation across a broad area along the West Coast. Specifically, this project developed a Multi-objective Optimization Framework that combined two assessments: (1) a 3D Seabird Collision Vulnerability Framework, which quantitatively evaluated the 2D and 3D density for all but the least observed seabird species, and (2) an Offshore Power Generation Model, which quantitatively evaluated offshore power generation capacity. Both assessments encompassed all waters in the study area that are shallow enough to support floating OSW mooring infrastructure (a depth of 1,300 m or less). The Optimization Framework maps' varying baseline risks of seabird-RSZ overlap, highlighting sites that would minimize seabird interactions with turbines while maximizing power generation. This framework also provides a mechanism to address uncertainties relevant to initial permitting needs.

This project provides insight into how seabirds intersect the RSZ in the vertical (third) dimension. Previous studies by Leirness et al. (2021), Russell et al. (2023), and others (such as Nur et al. 2011 and Adams et al. 2016) have advanced the understanding of the California Current System (CCS) seabird community by successfully pioneering 2D prediction efforts, but all of these miss the vertical component that is needed to better resolve questions regarding seabird propensity to utilize airspace that overlaps RSZ heights. Dynamic soaring species are expected to be particularly susceptible to overlap with RSZs, emphasizing the need to consider them in OSW permitting processes, especially as some are endangered.

To compare seabird density at RSZ-height with wind energy generation, several turbine build-out scenarios across a broad area of the West Coast were simulated. The OSW Power Generation Model, adapted from a Schatz Energy Research Center model (Severy et al. 2020), was combined with the 3D Seabird Collision Vulnerability Framework within a Multi-objective Optimization Framework. This allowed researchers to quantify tradeoffs between seabird density at RSZ heights and cumulative power generation potential for various scenarios in CCS waters from Point Conception, California to Newport, Oregon.

This report synthesizes key findings from four interim reports, which quantified the following metrics at regularly spaced intervals across the study area:

1. Full distribution of wind speeds (windscape)
2. Seabird collision vulnerability (defined here as densities predicted at or above 10 m as a proxy for RSZ-height)

3. Power-generation potential based on the windscape for various scenarios
4. Tradeoffs between seabird collision vulnerability and energy generation potential

The Project Deliverables section provides additional details regarding these interim reports. Insights gained from this study can help inform OSW project permitting, construction, and operational decisions. These findings should be useful in aiding agencies, developers, and other OSW stakeholders in making informed decisions that balance ecological considerations with renewable energy goals.

This project supports California's renewable energy goals while helping to minimize the potential for interactions between OSW developments and the distinct seabird community off California by developing an analytical framework to address uncertainties about the vertical structure of the seabird community, particularly those flying at RSZ-height, and how this interacts with the potential to generate renewable power using OSW. As OSW planning evolves, the Optimization Framework presented here can be adapted and applied to other regions, promoting explicit consideration of seabird populations when making landscape-level decisions regarding where to site OSW facilities.

The density of birds at RSZ-height (exposure to interacting with rotating turbine blades) is much greater than what is expected in terms of collision rates. Collision rates, which must be predicted on a site- and a project-specific basis, are influenced by multiple factors in addition to the presence and passage of birds at RSZ-height (vulnerability). These include physical aspects of the bird (size, speed, flight style), physical properties of the turbine (size, rotation rate), physical aspects of the interaction of birds and turbines at a site (bird approach angle relative to turbine angle, exact position of bird within the RSZ), and individual birds engaging in behaviors that might divert attention from navigation, thereby altering their ability to detect and avoid RSZs (foraging and transiting). This additional information, along with the currently challenging-to-predict responses of novel types of seabirds to the presence of wind turbines expected to be impacted by wind facilities in the OCS of California, is required to calculate reliable collision rates. What can be calculated at the present time, given the present information, is the rate of exposure of encountering RSZs.

CHAPTER 2: Project Approach

The project assessed tradeoffs between seabird collision vulnerability and offshore power generation capacity, necessitating development of a comprehensive Optimization Framework to integrate several semi-independent components (Figure 1). This framework used the extensive information already amassed about West Coast seabirds via various scientific aerial- and ship-based surveys between 1980 and 2006 to evaluate various offshore sites' optimality in balancing seabird conservation with power generation needs.

Figure 1: Framework to Assess Tradeoffs Between Seabird Collision Vulnerability and Offshore Power Generation Capacity

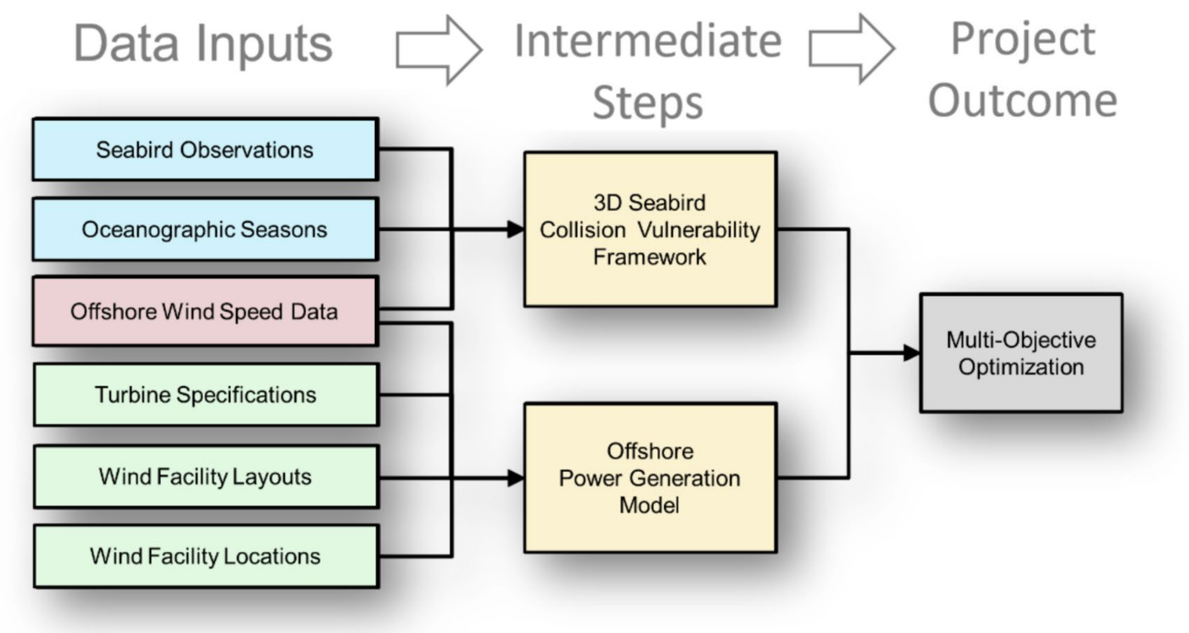

This Multi-objective Optimization Framework was conceptualized to evaluate the optimality of various offshore sites, in terms of their ability to balance seabird collision vulnerability with power generation needs (gray box). This overarching objective was achieved through two key assessments (yellow boxes): the 3D Seabird Collision Vulnerability Framework and an Offshore Power Generation Model. Data inputs supporting these assessments are color-coded as being specific to the 3D Seabird Collision Vulnerability Framework (blue boxes), specific to the Power Generation Model (green boxes), and shared inputs (pink box).

Source: Schatz Energy Research Center, H. T. Harvey & Associates

The Schatz Energy Research Center led the Multi-objective Optimization Framework analysis, the offshore windscape analysis, and the Offshore Power Generation Model. The 3D Seabird Collision Vulnerability Framework analysis was conducted by H. T. Harvey & Associates and the Schatz Energy Research Center, with R. G. Ford Consulting Company providing the standardized datasets supporting 2D seabird density estimates and H. T. Harvey & Associates providing the seabird flight height dataset.

Study Area

Final predictions encompassed the coastal and OCS waters of central and northern portions of the CCS, spanning from Point Conception, California, to Newport, Oregon (34.40°N to 44.74°N) (Figure 2). Seabird observations extended out to 370 kilometers (km) from the coastline (inclusive of the U.S. Exclusive Economic Zone), but optimization predictions are restricted to the upper portion of the slope (approximately 80 km) and landward. This more focused prediction region includes all upper OCS waters shallow enough to support the current OSW mooring technologies (that is, shallower than 1,300 m).

The CCS is a productive marine ecosystem due to the upwelling of nutrient-rich waters that support a diverse and abundant marine community, including seabirds. It serves as a crucial foraging ground for many seabird species, including those migrating seasonally to the CCS from waters around breeding grounds thousands of kilometers away (such as Hawaii and New Zealand). Dynamic soaring seabirds, such as albatrosses, petrels, and shearwaters, rely on winds for their flight to be energy-efficient, with faster winds facilitating travel that involves traversing greater ranges of altitudes above the sea surface. It is thought that this flight style makes certain seabird species particularly likely to achieve RSZ-height in adequate winds.

Thirty-two wind facility location and build-out scenarios were simulated for eight reference areas (Figure 2). Build-out scenarios for each reference area included 12-megawatt (MW) or 15-MW turbines in various arrays, designed to fully utilize the area, create a 600-MW facility, or follow specific developer plans.

These reference areas included two leased BOEM Wind Energy Areas (WEAs) (Humboldt and Morro Bay), one previously designated Call Area (Diablo Canyon), which existed at project initiation, and five additional areas of interest. The non-WEA areas included two notional areas — one off the coast of Crescent City (Pacific Ocean Energy Trust 2021) and one off Cape Mendocino — as well as a proposed area in California waters offshore of the Vandenberg Space Force Base, specifically the CADEMO project (California State Lands Commission 2021).

To broaden the understanding of seabird vulnerabilities, optimization outputs were generated for two additional reference areas: the Delgada Canyon and the Monterey System submarine canyons. These areas were selected due to their status as likely ‘hotspots’ of seabird activity, including deeper-water seabirds. Submarine canyons have unique circulation properties that generate localized areas of upwelling and productivity (Croll et al. 2005), resulting in some of the greatest concentrations of seabirds off California (Nur et al. 2011). These submarine canyon reference areas bookend optimization outputs, as they were predicted to be the locations where seabird densities at RSZ-height are maximized. While these locations are likely to pose greater risks to seabirds, there is no expectation that wind facilities would be developed in these locations; they are included only for illustrative purposes.

Figure 2: Study Area for Assessing Tradeoffs Between Seabird Collision Vulnerability and Offshore Power Generation Capacity

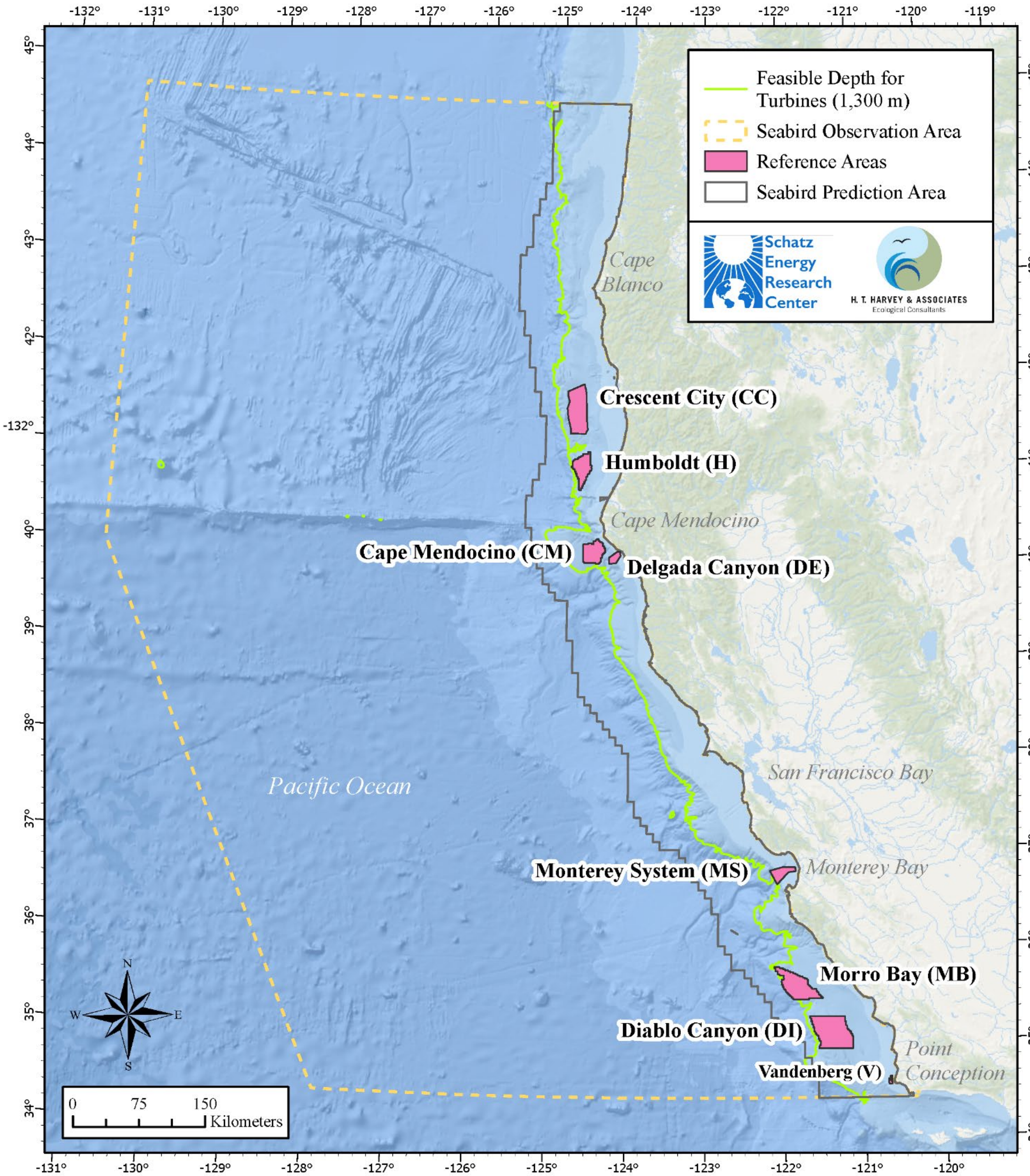

The seabird observation boundary (dashed yellow line) delineated the entire area for which seabird observations were amassed and standardized to support development of 2D predictions via the 3D Seabird Collision Vulnerability Framework. The California Current System occupies the length and breadth of this area. This observation boundary also extended as far westward as the U.S. Exclusive Economic Zone. In contrast, the seabird prediction boundary (solid grey line) delineated the more focused spatial extent of 2D and 3D density predictions, including all areas being considered for commercial OSW developments off California. The 1,300-m feasible depth line (green) represents the western extent of where turbines are expected to be potentially deployable off California, given state-of-the-art mooring technologies. Reference areas (pink polygons) include BOEM WEAs

(Humboldt, Morro Bay), a Call Area existing at the outset of this project (Diablo Canyon), two notional areas for potential future wind development (Crescent City, Cape Mendocino), a developer-proposed site (Vandenberg), and submarine canyons where deep-water seabirds are known to concentrate (Delgada Canyon, Monterey System). BOEM also designated WEAs in Oregon, but these were not assessed in this study.

Source: Schatz Energy Research Center, H. T. Harvey & Associates

Study Seasons

Wind and water circulation patterns affecting seabird behavior and community composition vary throughout the year. The 3D Seabird Collision Vulnerability Framework, therefore, assessed seabird density and vulnerability separately for three oceanographic seasons derived from predictable, seasonal shifts in wind patterns and sea surface temperatures:

- Upwelling (February 25 to August 13): Features strong northwest winds that, with the effects of the earth’s rotations, bring nutrient-rich deep water to the surface, boosting ocean productivity and supporting seabird foraging.
- Oceanic (August 14 to November 20): Features reduced wind speeds, allowing warmer subtropical waters to move into the CCS, attracting warmer-water migrants.
- Davidson Current (November 21 to February 24): Features the surfacing of the northward-flowing Davidson Current, which brings warmer, less productive waters. Winter storms, with their southerly winds, further strengthen surfacing of this current.

Windscape Analysis

Understanding wind patterns is crucial for assessing seabird behavior and OSW power generation potential, thus a windscape analysis was conducted to support the 3D Seabird Framework and the Offshore Power Generation Model. The likelihood of seabirds flying at heights greater than 10 meters varies as a function of seabird flight style and of wind speed, the latter of which also affects wind turbine efficiency and capacity.

This project analyzed wind data from the CA-20 and Northwest Pacific modeled wind speed assessment provided by the National Renewable Energy Laboratory (NREL 2023). These data, covering 2000 to 2019, captured wind speeds at a 5-minute time interval at various altitudes above sea level (ASL). For practicality, wind data from 10 meters, 120 meters, 140 meters, and 160 meters ASL were downscaled to 15-minute time intervals as a way to balance detail with data volume and computational complexity.

Specifically, the full distribution of wind speeds was quantified and predicted for thousands of regularly spaced locations (that is, grid cells). To support the 3D Seabird Framework, wind speeds expected at 10 m ASL were used to match where wind speed measures were taken by ship-based observers for the seabird flight height dataset. To support the Offshore Power Generation Model, the same analysis was conducted but based on wind speeds expected at rotor-hub heights (150 m ASL), to determine power generation capacity.

Estimating Seabird Collision Vulnerability

The 3D Seabird Framework integrated various analyses to predict the composition and density of California's seabirds, particularly those vulnerable to collision with turbine blades due to their flight heights.

3D Seabird Collision Vulnerability Framework

The 3D Seabird Framework (Figure 3) is best understood as a three-component analysis within the broader Optimization Framework:

- Component I: Relate Flight Heights to Wind Speed — The diverse seabird community of the CCS was divided into flight groups (FGs), or groups of species having distinct flight styles, with style being a function of their morphology as proposed by Ainley et al. (2015). FG-specific probability curves were generated to indicate the likelihood of seabirds flying at RSZ heights inclusive of the full spectrum of wind speeds in which turbines will rotate. This was modeled using a mixed-effects logistic regression on an extensive seabird flight-height behavior dataset.
- Component II: Predict Densities in 2D — Seabird observation data were partitioned among the three oceanographic seasons. Traditional 2D density predictions were made at regularly spaced intervals for each species and season. Doing this required applying a spatial interpolation algorithm to an extensive seabird presence and abundance datasets generated by at-sea surveys conducted across the region from 1980 to 2016.
- Component III: Convert 2D Densities to 3D — The 2D density predictions were converted to a 3D representation. This involved:
  - Step 1: Generating comprehensive distributional representation of the windscape (including extremes) for each season and location.
  - Step 2: Integrating this windscape with Component I outcomes to derive seasonal-, site-, and FG-specific probabilities of being at collision risk height (greater than 10 m ASL).
  - Step 3: Applying these probabilities to the 2D density estimates to partition overall 3D densities and isolate the predicted 3D density at RSZ-height.

Post-prediction, spatially explicit 2D and 3D seabird densities were aggregated by season and species, then visualized via mapping. Annual prediction maps represent long-term, multi-decadal perspectives of the seabird community, relevant to the timescale of OSW facilities, which are typically permitted to operate for decades.

Figure 3: Analysis Components of the 3D Seabird Collision Vulnerability Framework

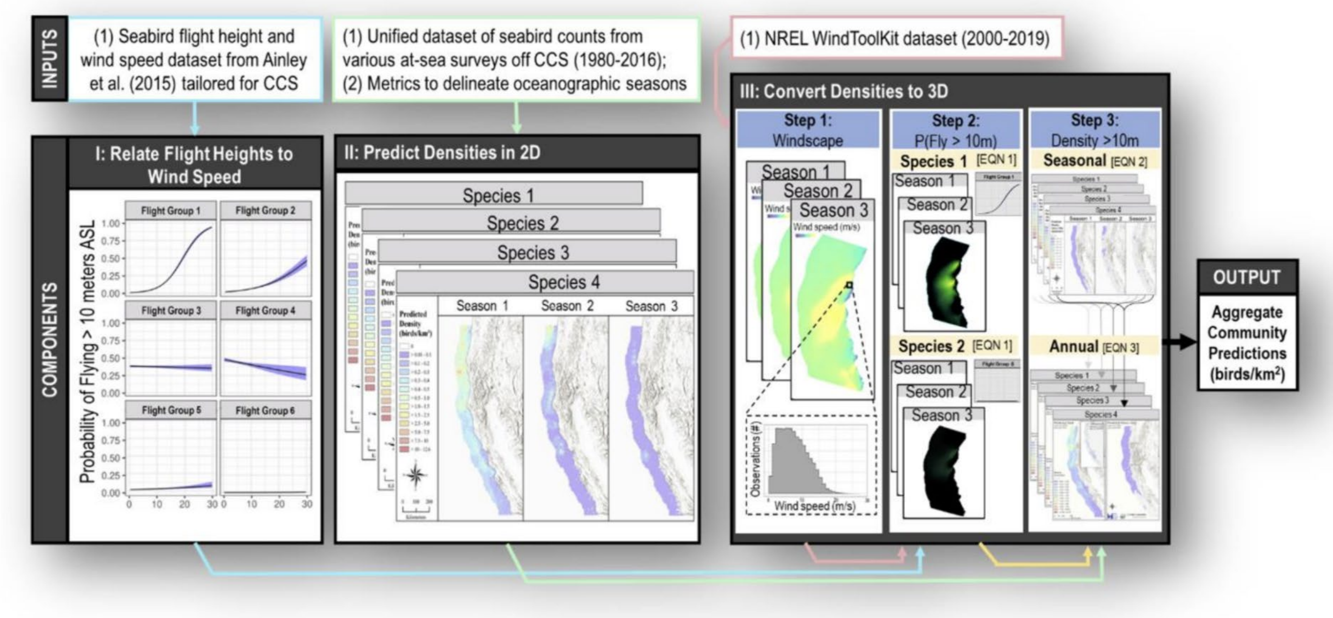

The flowchart of the 3D Seabird Collision Vulnerability Framework illustrates how diverse data were input and integrated across the three analysis components to generate seasonal and annual predictions of 3D density (birds per km²) for California's seabird community. Each panel corresponds to a distinct component, with colored arrows depicting data flow and connections between components.

Definitions: NREL: National Renewable Energy Laboratory; m/s: meters per second; EQN: equation.

Source: H. T. Harvey & Associates

Flight Height and Wind Speed

The offshore NREL 15-megawatt reference turbine RSZ currently spans from 30 m ASL at its lowest extent to 270 m at its highest extent (Gaertner et al. 2020). For this study, birds vulnerable to collision were defined as those observed flying at heights of 10 m or greater. While 10 m does include airspace below the lower extent expected for OSW turbines at 30 m ASL, it was necessary to use this more inclusive threshold due to how the original flight height data were collected by flight-height bin. However, it should be noted that observations occurring at the same time as the binned flight-height data indicated seabirds flying above, and in some cases well above, 30 m ASL (Ainley, pers. comm.). These observations are further supported by recent autonomous thermal tracking technology in the Humboldt WEA (Schneider et al. 2024a).

Probabilities of seabirds flying at heights that increase their potential to overlap with RSZs (above 10 m) were computed across a range of OSW speeds from 0 meters/second (m/s) to 30 m/s (inclusive of all wind speeds required for turbine rotation, which are 3 m/s to 25 m/s [Severy et al. 2020]). These probability estimates were based on data specifically tailored to seabirds present in the CCS, sourced from a comprehensive assessment covering a significant portion of the eastern Pacific Ocean, including the CCS (Ainley et al. 2015).

To generate probability curves of seabirds flying at RSZ heights for various FGs and wind speeds, an extensive dataset collected between 1976 and 2006 was used. This dataset was filtered to retain all observations from the CCS and included species known to be present off California but also observed elsewhere (such as Laysan albatross observed in the Equatorial Pacific). A key aspect of these data collection efforts involved categorizing flight heights for all seabird observations into the following predefined categories or bins:

- On the sea surface
- Flying 0 m to 3 m ASL
- Flying 3 m to 10 m ASL
- Flying above 10 m ASL

The predicted probability of flying above 10 m for each flight-style group, with wind speeds as a predictor, was calculated using a mixed-effect logistic regression, a statistical model to predict how likely birds are to fly above 10 m for different flight styles, depending on wind speed. Confidence intervals about the model predictions were generated via nonparametric bootstrapping, a resampling method to check how much the results might vary given different samples of the data.

Seabird Density Predictions in 2D

Extensive datasets from nine at-sea strip-transect aerial and vessel-based seabird surveys in waters off California and Oregon (1980–2016) were made consistent and combined to support the 3D Seabird Framework (Figure 4). Despite slightly varied methods, all surveys adhered to continuous strip-transect observations typical of at-sea seabird surveys (Spear et al. 1992, 2004). Observations were standardized to 1-square-kilometer (km^2) units of survey effort to account for differences in strip-widths and lengths, ensuring that spatial efforts associated with counts were based on equivalent levels of effort. Counts were then corrected for the movement direction and speed of seabirds relative to observers (Spear et al. 1992) using established methods that have been previously published (such as Clarke et al. 2003 and Ford et al. 2021).

Density predictions in 2D were derived using inverse distance weighting, a spatial interpolation algorithm that assigns weights based on distance from observed points to prediction points. Density estimates (birds per km^2) for each species-season combination were generated across a uniform 5-minute-latitude by 5-minute-longitude spatial grid.

Figure 4: Seabird Survey Effort Across the Entire Observation Area

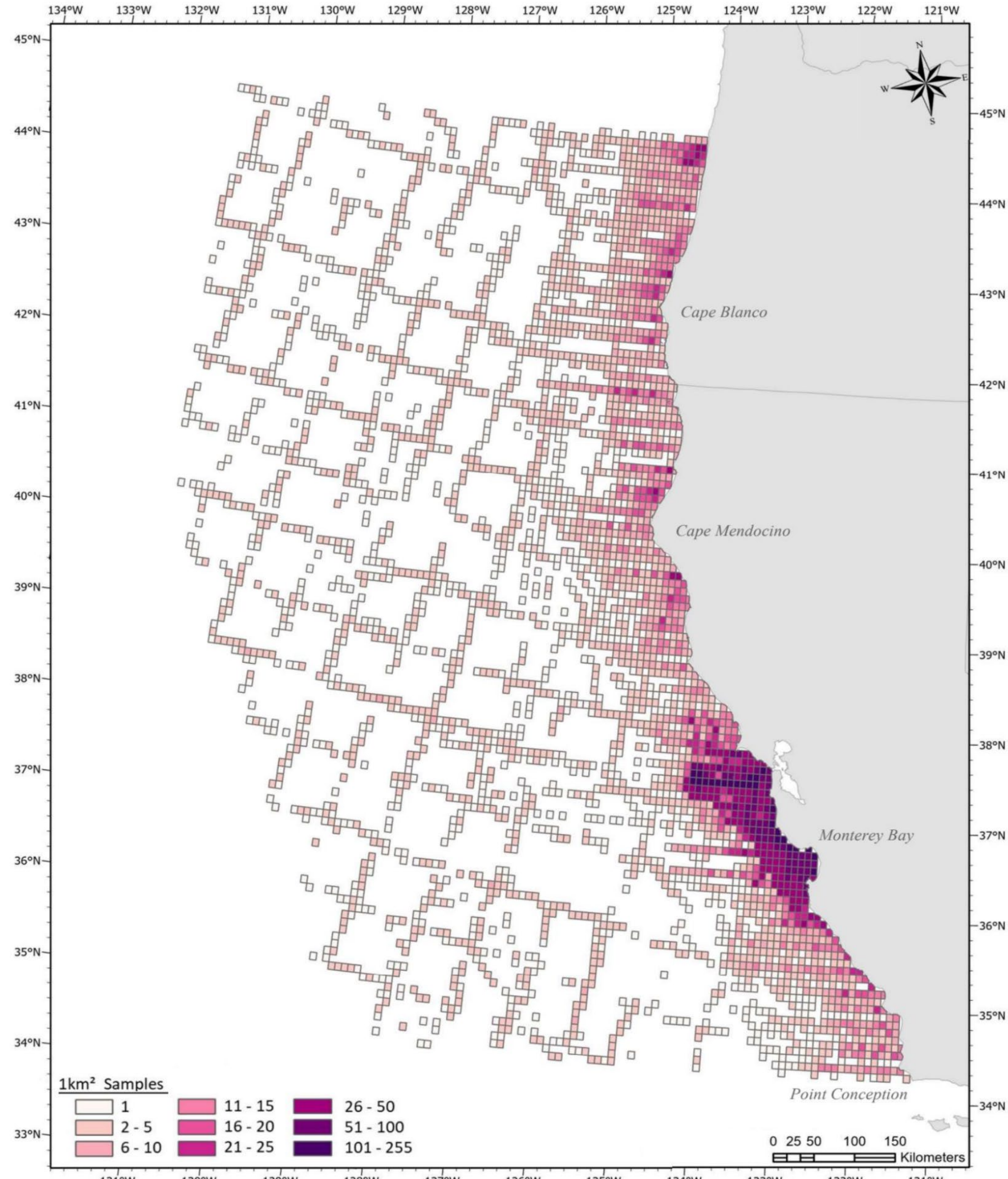

Predictions made from these survey data were confined to an 80-km band stretching westward from the coast. The intensity of the survey effort is indicated using a color gradient, with darker shades indicating areas with a greater number of equal-area (1 km²) units of at-sea survey effort.

Source: H. T. Harvey & Associates

Converting Density Predictions from 2D to 3D

The final component provided species-specific estimates of seabird density above 10 m ASL (Figure 5). This 3D conversion integrated:

- Component I: Response curves for each FG describing the probability of flying above 10 m based on wind speed.
- Component II: 2D density estimates for all seabird species observed in at least 100 km2 of at-sea survey effort. This eliminated rarely observed birds from the assessment.
- Component III: Probabilities of flying above 10 m given the windscape for each grid cell.

Figure 5: Integrating the Windscape Into Site-Specific Predictions of Seabird Densities at Rotor Swept Heights

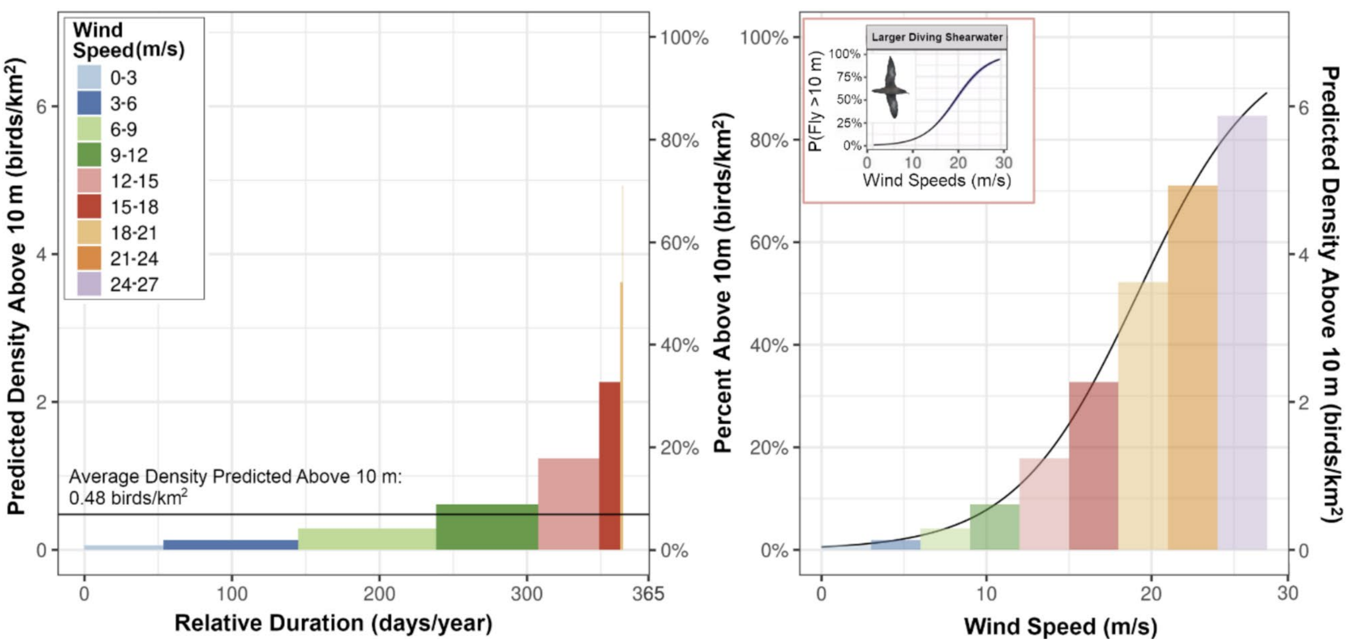

This figure demonstrates how wind speed data were used to predict seabird densities at the heights at which they could encounter wind turbine rotor-swept zones (Component III of the 3D Framework; see Figure 3), using calculations for sooty shearwater in the Humboldt WEA as an example. Wind speeds were hindcast at each prediction site for each 15-minute interval over a 20-year period (2000–2019). These measurements were grouped into 0.5-m/s increments to capture the full range of wind conditions. These detailed wind data were then applied to models predicting the likelihood of seabirds flying above 10 m. For example, in the Humboldt WEA, it is predicted that, based on long-term historical data, an average of 0.48 sooty shearwaters per km² would be flying above 10 m in this WEA, or approximately 7 percent to 8 percent of the predicted population at this location (range: 0-85 percent).

Source: Schatz Energy Research Center

2D Versus 3D Perspectives

Community Composition: To assess differences in the composition of California's seabird community from 2D (all elevations) and 3D (above 10 m) perspectives, the study area was divided into six regions, with a prominent oceanographic feature, Cape Mendocino (40.44°N), serving as the boundary between the northern and the central CCS. The east-west divisions were determined by distances from the coastline: near (0–3 nautical miles [nm]), intermediate (3–20 nm), and offshore (greater than 20 nm). These divisions take into consideration changes in regulatory jurisdiction as the distance from land increases, as nearshore waters are under state jurisdiction whereas intermediate and offshore waters are under federal jurisdiction. The subdivision of federal waters into intermediate and offshore waters allowed for community composition to be quantified separately for offshore waters currently being considered for wind-energy development (greater than 37 km [20 nm]) versus intermediate waters, which are not being considered for wind energy developments at this time.

Density: To assess differences in the density of California's seabird community from 2D and 3D perspectives, prediction maps depicting the density of seabirds expected at all elevations versus above 10 m ASL were generated.

Estimating Power Generation Potential

NREL's wind toolkit dataset (CA-20 and Pacific Northwest versions) served as the starting point for estimating potential energy generation from wind turbines (see Windscape Analysis section). This data set provides expected wind speeds at the hub height of turbines, representing a time series of wind speeds used, along with the turbine power curves (Figure 6), to generate power generation estimates per turbine at a 15-minute interval for a 12-MW and a 15-MW turbine.

Figure 6: Power Curves for Two OSW Turbines

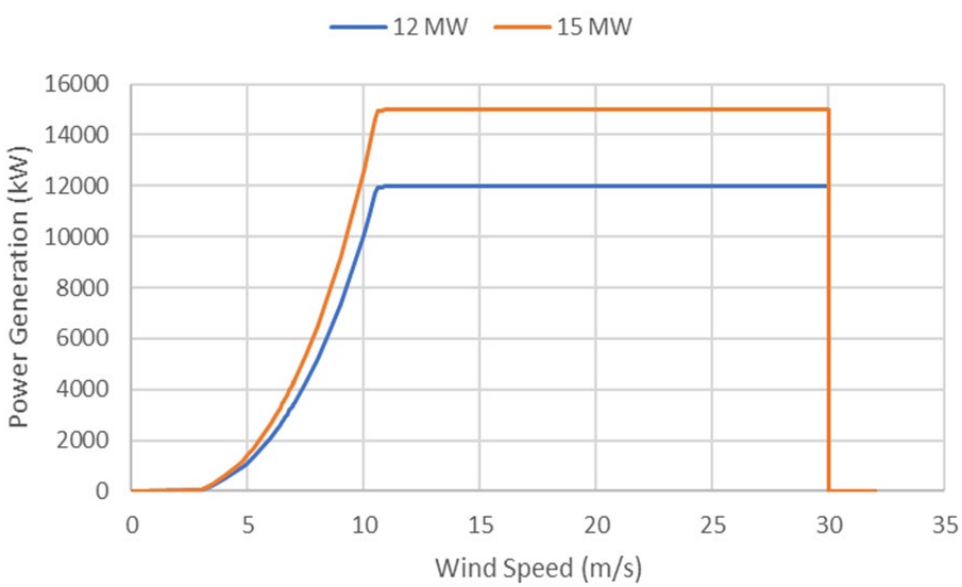

This figure shows the power generation curves for the 12-MW and the 15-MW OSW reference turbines used in the study. The curves illustrate how power output (in kW) increases with wind speed (m/s) until reaching the rated capacity of each turbine.

Source: Beiter et al. 2020

Scenarios Simulated

Regional

To assess power generation across the entire region of interest, generation expected from a single turbine was simulated at the center of each cell of a high-resolution grid from NREL's WIND Toolkit dataset covering the study area. This NREL-generated grid was then downsampled from 2-km grid cells to match the seabird prediction grid (5 minute by 5 minute). Although 12- and 15-MW turbines were both simulated for this, results reported here are restricted to the 12-MW simulations, as the key takeaways did not differ from that of the 15-MW simulations. The purpose of this single turbine scenario was to show the range of values available in the study area and as an input to the full coast optimization analysis.

Reference Areas

In addition to single-turbine generation scenarios, larger multi-turbine wind facility scenarios were also assessed (Table 1). These scenarios included both a 600-MW buildout and a full buildout for each of the eight reference areas described in the study area section. While most of these locations were selected for their potential to host OSW facilities, the submarine canyon reference areas were selected to represent sites with relatively high densities of seabirds and give a better understanding of the range of potential bird vulnerability values. Full buildout is defined as the maximum number of turbines that could be installed in the area, given staggered rows of turbines spaced at 7 x 10 turbine rotor diameters (Figure 7). The 600-MW scenarios occupy a subarea of the reference areas that was adequate to host this nameplate capacity.

Table 1: Sizing of Full Buildout for Relevant Scenario Locations

Location Name	Abbreviated Name	Turbine Nameplate (MW)	Number of Turbines	Total Nameplate Capacity (MW)
Crescent City	CC	12	363	4,356
Crescent City	CC	15	292	4,380
Humboldt	H	12	176	2,112
Humboldt	H	15	142	2,130
Cape Mendocino	CM	12	182	2,184
Cape Mendocino	CM	15	146	2,190
Morro Bay 376[1]	MB	12	318	3,816
Morro Bay 376	MB	15	253	3,795

[1] The Morro Bay area underwent revisions during the BOEM planning process. For this study, Morro Bay 376 designates the final boundary configuration of the WEA used by BOEM for leasing in 2022, which contained 376 square miles.

Location Name	Abbreviated Name	Turbine Nameplate (MW)	Number of Turbines	Total Nameplate Capacity (MW)
Diablo Canyon	DI	12	494	5,928
Diablo Canyon	DI	15	397	5,955

Source: Schatz Energy Research Center

Figure 7: Minimum Spacing Between Turbines for The Full-buildout Scenarios

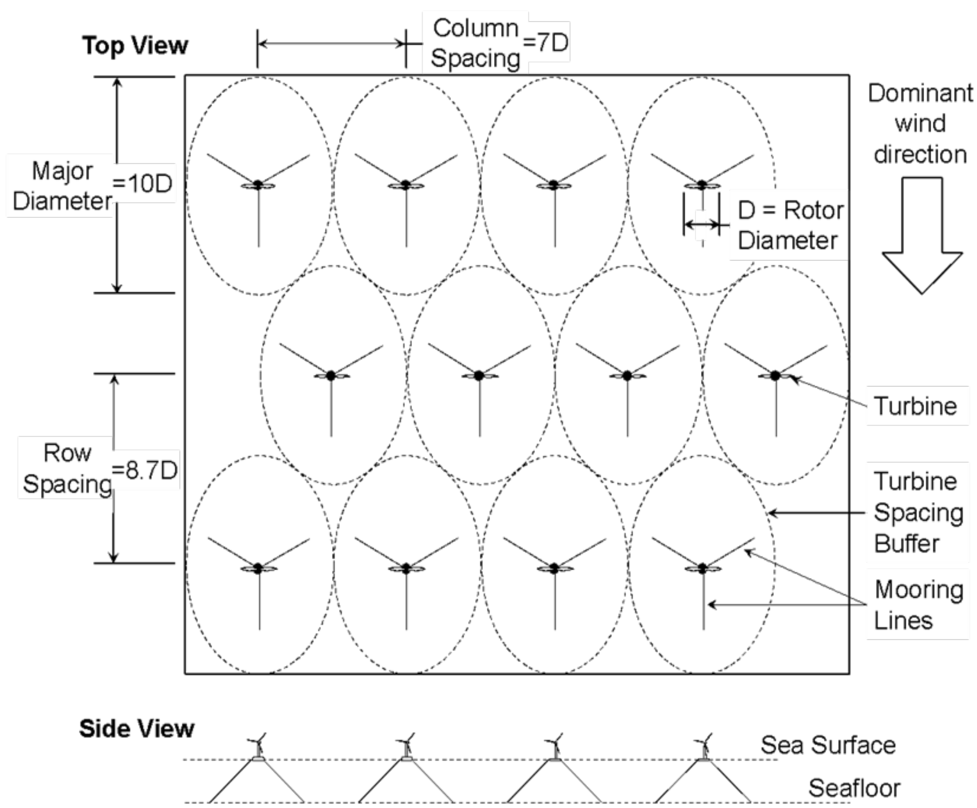

Source: Severy et al. 2020

Loss Factors

Initial power estimates were downrated based on several loss factors. These loss factors were divided into three broad categories: proportional losses, shutdown losses affecting single turbines, and shutdown losses affecting the entire wind facility.

Proportional Losses: Proportional losses are small, consistent reductions in power generation that result from various sources and affect all turbines in the wind facility (Table 2). These losses were included in the model as a downrating for power generation at all time steps and were based on the experiences of terrestrial wind power facilities (AWS Truepower 2014). Wake losses, influenced by wind facility geometry and environmental factors (particularly wind direction), were also treated as proportional losses and estimated using NREL's eddy-viscosity model (Freeman et al. 2014).

Turbine-related Shut-down Losses: Turbines shut down for a variety of reasons, ranging from environmental conditions to routine maintenance and mechanical failure (Table 2). To account for these factors, a binomial distribution was used to randomly select turbines and times to be treated as 'shutdown' time (that is, power generation set to zero) for the proportion of time that shutdowns are likely to occur, based on failure rates at terrestrial wind power facilities (AWS Truepower 2014).

Transmission-related Shut-down Losses: Shut-down losses prevent the entire wind power facility from providing power to the grid, which can occur in a few circumstances (Table 2). These transmission-related shut-down losses were modeled using a binomial distribution to select time steps when the entire facility would be unable to generate electricity. The probability of these failures was informed by terrestrial wind power facilities (AWS Truepower 2014).

Table 2: Loss Factors Included in Power Generation Simulation Scenarios (Percent)

Category	Origin	Typical	Lower	Upper
Proportional	Electrical Efficiency	2.0	-	-
Proportional	Power Consumption of Weather Package	0.1	-	-
Proportional	Sub-optimal Operation	1.0	-	-
Proportional	Power Curve Adjustment	2.4	-	-
Proportional	Inclined Flow	0.0	-	-
Proportional	Blade Degradation	1.0	-	-
Proportional	Wake Loss (Calculated)	-	1.6	5.1
Turbine	Contractual Turbine Availability	3.0	-	-
Turbine	Non-contractual Turbine Availability	1.3	-	-
Turbine	Availability Correlation With High Wind Events	1.3	-	-
Turbine	Site Access	0.1	-	-
Turbine	Lightning	0.1	-	-
Turbine	Directional Curtailment	0.0	-	-
Turbine	Environmental Curtailment	0.0	-	-
Turbine	Purchase Power Agreement Curtailment	0.0	-	-
Transmission	Availability of Collection and Substation	0.2	0.2	0.4
Transmission	Availability of Utility Grid	0.3	0.3	0.6
Transmission	Plant Restart After Grid Outages	0.2	0.2	0.4

This table summarizes the loss factors considered in power generation simulations for OSW projects. The factors are categorized into proportional, turbine-related shutdown, and transmission-related shutdown, showing typical percentage loss values and applicable ranges. These factors affect the overall efficiency and reliability of OSW turbines.

Source: AWS Truepower 2014

Assessing Tradeoffs Between Seabird Vulnerability and Generation Potential

Each site is expected to have a different balance of seabird vulnerability and power generation potential. Some sites may exhibit small vulnerability but also small power generation potential, while others may have great vulnerability and small power output, or great vulnerability and great power output. None of these scenarios are ideal. The optimal OSW sites with respect to seabird protection are ones with relatively small seabird densities at RSZ-height and relatively great power generation potential. Note that many other factors beyond seabird vulnerability and energy generation potential must, of course, be considered when selecting OSW sites.

To identify these sites, the Pareto optimization approach was used. This approach is detailed in the section in Chapter 3 titled "Optimization Framework and Pareto Front Curves: Interpretation of the Pareto Front." Although seabird density estimates were generated on a species-by-species basis, this final optimization assessment focused on aggregates. In addition to the overall community, the results for seabirds predicted to be particularly abundant above 10 m and those of regulatory importance are also presented. A full list and additional details about each species included in the Optimization Framework has been summarized (Appendix A, Table A-1). Aggregates presented are:

- All seabirds in the framework: The 44 most widely encountered seabird species, based on multi-decadal observations at-sea, are presented to facilitate an assessment of potential impacts inclusive of the broader seabird community. This approach captures the diversity of species and the existing range of flight strategies among various FGs, providing a look at how birds might be using this airspace given the best available knowledge.
- Sooty shearwaters: These seasonally resident seabirds travel vast distances from Southern Hemisphere nesting islands to the notably productive CCS, where they become the most abundant species in the CCS to feed. To some degree, they follow the seasonal peak of upwelling as it shifts northward, more abundant first in the south and then in the north. Their abundance and their likelihood to achieve the requisite heights is strongly tied to wind speeds, with the likelihood of overlapping RSZ-height increasing dramatically with increased wind speeds.
- Gulls: As a group, the nine gull species are collectively quite prevalent and have a propensity to fly at altitudes overlapping RSZ-height. Resident gull species tend to occur nearshore, whereas migratory gulls tend to follow the shelf-break in waters farther offshore (that is, traveling along the shelf-break). Their overall abundance, combined with their propensity to fly at various heights across all wind speeds, makes this group a dominant component of the community above 10 m.
- Federal and/or state Endangered Species Acts (ESA)-listed species: Species listed under the federal and/or state ESAs are legally protected due to their risk of extinction. Assessing these species' collision risks is vital to comply with legal requirements and conservation goals.

CHAPTER 3: Results

Windscape

The windscape analysis was crucial for understanding wind patterns relevant to seabird movement and OSW energy generation potential.

Wind Patterns Relevant to Seabird Community Predictions: The windscape exhibited obvious seasonal variability (Figure 8). Large-scale wind patterns and the resulting changes in ocean condition are major drivers of ocean circulation, productivity, and variation in seabird community composition and density. Different seabird species, with their varying body shapes, flight style, and energetic constraints, respond differently to these wind patterns. As explored in the following section on seabirds, these variations complicate predictions of how the windscape affects seabirds at RSZ-height.

Wind Patterns Relevant to Power Generation Predictions: From a power generation perspective, the fastest overall wind speeds were observed further offshore, particularly west of Cape Mendocino. These areas, with their fast and reliable winds, represent prime locations from a wind energy generation standpoint. In contrast, nearshore sites had slower wind speeds, reducing their suitability for large-scale wind facilities.

Figure 8: Offshore Windscape for Each Seabird-centric Oceanographic Season

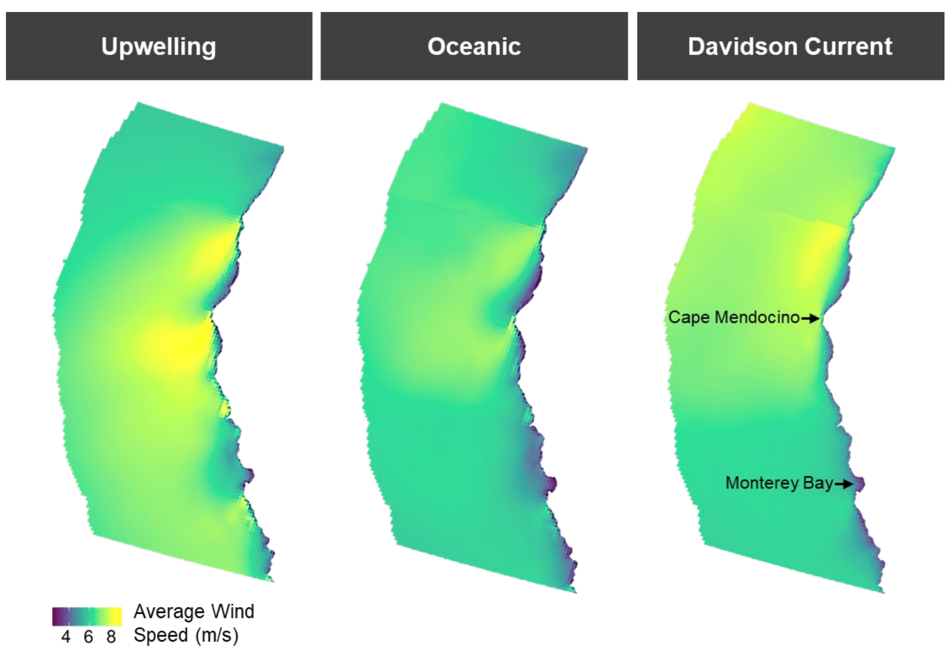

These twenty-year average wind speeds (2000–2019) at turbine hub height (150 m ASL) off California were derived from CA-20 and Northwest Pacific wind speed models.

Source: Schatz Energy Research Center, H. T. Harvey & Associates; derived from NREL 2023

Seabird Community

Flight Groups and Species Included: The seabirds included in this Multi-objective Optimization Framework represent a diverse and significant portion of California's seabird community, spanning 18 distinct FGs. In the at-sea surveys conducted from 1980 to 2016, 109 seabird species were observed. Of these, 44 species were included in the framework (Figure 9), based on their presence in at least 100 km² of the seabird observation dataset. For information regarding the species observed but not included in the framework, see Schneider et al. 2024b.

This large sample of seabird species ensures that the framework's aggregate predictions could encompass the core seabird community, accounting for resident and migratory species, as well as both widespread and localized species. While rare species are prioritized by regulatory and permitting processes, this framework highlights the most abundant and some of the rarer members of the seabird community. Abundant species, like the migratory sooty shearwater and the nonmigratory common murre, are included; together, these constituted over half of all seabirds encountered in the study area. Also included are less abundant and more localized species, such as the very coastal marbled murrelet (listed as California endangered and federally threatened).

Importance: Focusing on the most numerous species, the framework's predictions encompass much of the seabird community diversity and most of the individuals. The remaining 65 species that were observed but not included in the framework were so rare that their inclusion or exclusion would not have any consequential impact on the community-level optimization outcomes. This comprehensive approach allows for more reliable and relevant predictions about the impacts on the broader seabird community, without giving undue preference to any single species.

Figure 9: Seabirds Included in the Framework Organized by Flight Group

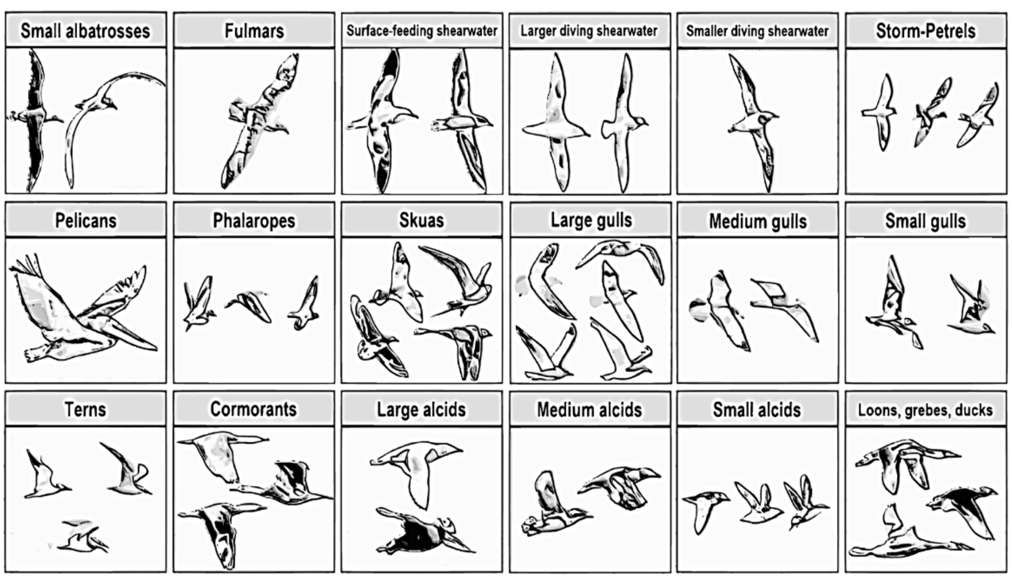

This figure illustrates the 18 distinct seabird flight groups included in the study, highlighting the diversity in species and flight styles. Each panel displays representative species for each flight group.

Source: H. T. Harvey & Associates

Probability of Flying at Collision Risk Height

This analysis highlighted the variable nature of seabird responses to wind speeds, which is critical for assessing collision risks with wind turbines. Although previous studies have generated 2D-density predictions, this study provides a novel mechanism to link seabird 2D-density estimates with their vertical use of airspace, adding a third dimension to the results. To predict the probability of seabirds flying above 10 m — a conservative proxy for the lower extent of the RSZ — the team analyzed 74,802 observations of seabirds flying at various heights and wind speeds across 18 distinct FGs.

Community-level Findings: For the collective seabird community, the likelihood of a bird flying above 10 m ASL was found to increase by a factor of 1.08 for every 1 m/s increase in wind speed (logistic regression, $P < 0.001$, df = 76,367).

Seabird Flight Group Findings: When examining flight height by FG rather than by the aggregate community, significant variability in responses to increased wind speeds was found (Figure 10). Coefficients associated with the FG-specific regressions are available in Schneider et al. (2024b). These patterns highlight the diversity in seabird flight responses to wind speed variations:

- Vulnerability increased as wind speeds increased:
    - Largest response: larger diving shearwaters
    - Strong response: small albatross; surface-feeding shearwaters; pelicans; and loons, grebes, and ducks
    - Moderate response: fulmars, skuas and jaegers, and large alcids
- Vulnerability was constant across all wind speeds:
    - Negligible probability of flying above 10 m: smaller diving shearwaters, storm-petrels, phalaropes, cormorants, medium alcids and small alcids
    - Moderate probability of flying above 10 m: large gulls, medium gulls
- Vulnerability decreased as wind speeds increased:
    - Small gulls, terns

Figure 10: Probability of Flying at Least 10 Meters Above the Sea Surface as a Function of Wind Speed

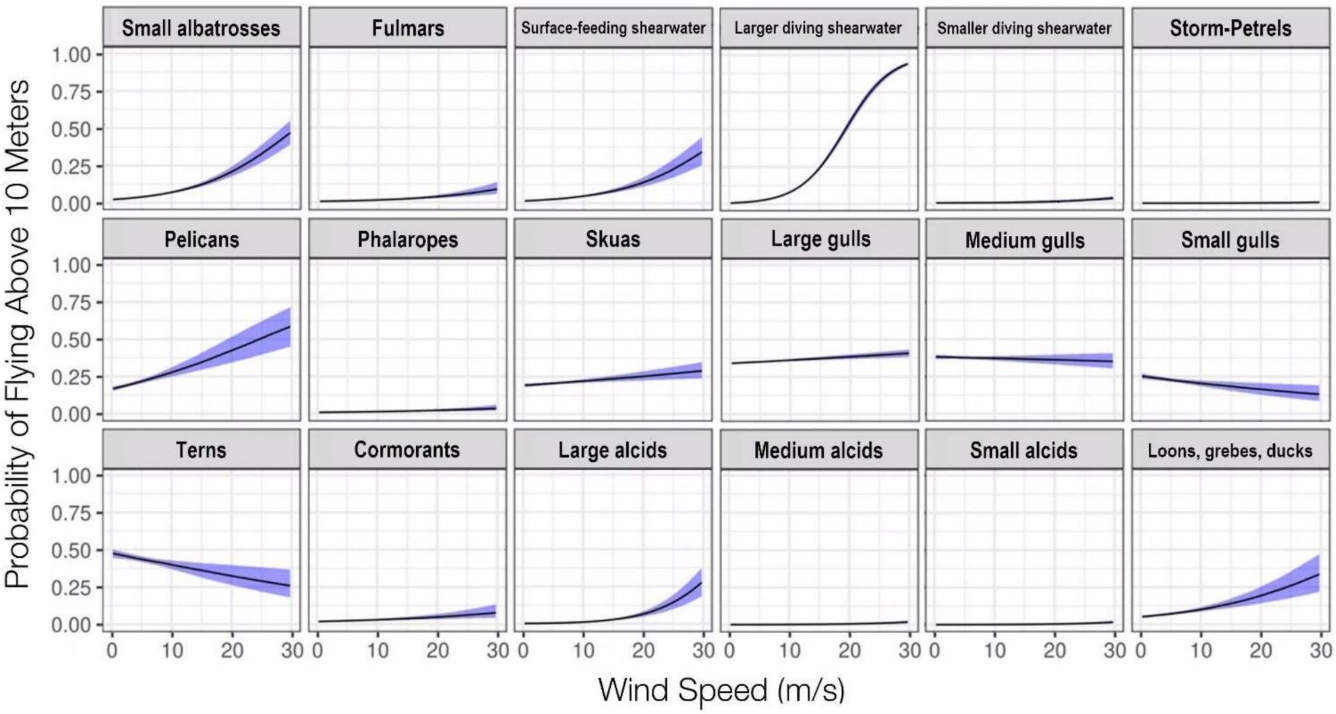

This figure shows the predicted probability of seabirds flying 10 m or more above the sea surface at varying wind speeds (m/s) for each flight-style grouping. Data and predictions encompass the full range of wind speeds needed for turbine rotation (3 to 25 m/s). Shaded regions about each line depict 95-percent confidence intervals.

Source: H. T. Harvey & Associates, Schatz Energy Research Center

2D Versus 3D Perspectives

The seabird community composition varied when assessed from a 2D (all elevations) versus a 3D (above 10 m) perspective (Figure 11).

Broad Patterns

The density and composition of the seabird community varied most notably in the vertical dimension (2D versus 3D). When comparing the seabird community present at all elevations to seabirds present above 10 m, the key takeaways are:

- The order of magnitude reductions in seabird densities above 10 m: There are significant reductions in the predicted densities of seabirds above 10 m.
- The dominance shift from alcids and shearwaters below 10 m to gulls and shearwaters above 10 m: Predictions inclusive of all seabirds, both below and above 10 m, suggest a seabird community dominated by alcids (30-40 percent of the entire community) across all regions. However, when predictions are restricted to 10 m and above, species composition is much different. Alcids become less prevalent with increasing distance from the sea surface, comprising a maximum of about 5 percent of the total population above 10 m, while gulls become much more prevalent, comprising about 60 percent of

the total population above 10 m across all regions. Shearwaters remain a consistent presence both below and above 10 m, making up about 15–30 percent of the total population across all regions and elevations. Loons, grebes, and ducks are another major component of the seabird community at all elevations and above 10 m, especially in state waters. All other seabird groups included in the framework (including phalaropes, cormorants, pelicans, and storm-petrels) only comprise about 15 percent of the community at all elevations and about 5 percent of the community above 10 m ASL, making them less vulnerable to collision.

- Reduced Diversity Above 10 m: The community composition above 10 m has fewer species compared to the overall community, inclusive of birds flying below 10 m ASL. The 2D perspective includes significant contributions from alcids, storm petrels, cormorants, and phalaropes.

Above 10 Meters

Seabird densities expected above 10 m are consistently less than the density of seabirds considering all elevations (2D). This can be seen by comparing the birds per km^2, provided in brackets above each bar in Figure 11, at all elevations versus those above 10 m. Taxa were grouped broadly for clarity, with average annual density estimates (birds per km^2) provided above each column. The most notable differences in composition were between nearshore and more distant waters. In nearshore waters there was a greater prevalence of loons, grebes, and ducks, with shearwaters being more prevalent in intermediate and offshore waters.

Importance: Overall, these conclusions highlight the importance of vertical distribution in understanding seabird community composition and assessing the potential impacts of OSW energy development on different seabird species.

Figure 11: Seabird Community Predictions Overall Versus Above 10 Meters

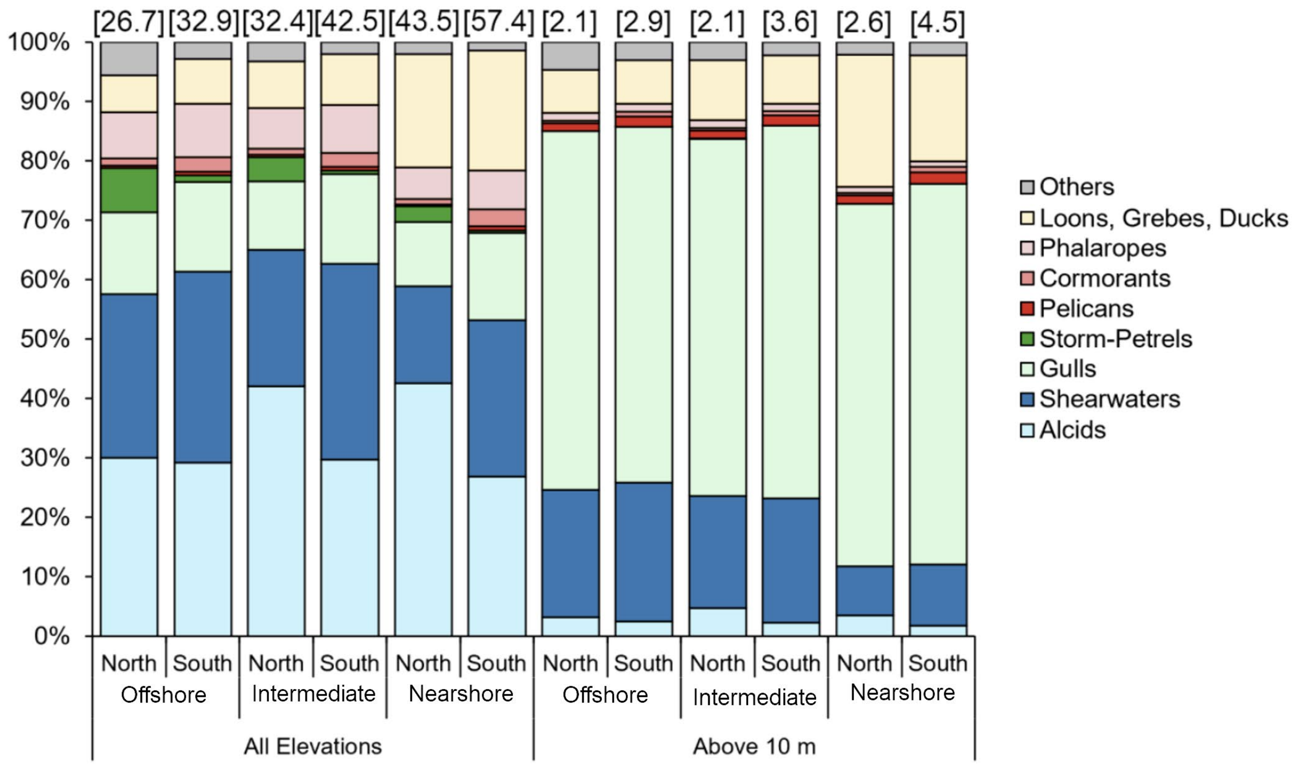

This figure illustrates the composition of California's seabird community from both 2D ("All Elevations") and 3D ("Above 10 m") perspectives across six regions, categorized by geographic location (north and south of Cape Mendocino) and distance from the coastline (offshore, intermediate, nearshore). Each bar represents the average annual density estimates (birds per km²) for all seabird taxa included in the Multi-objective Optimization Framework, and the average densities of the seabird community aggregated at each unique region and elevation are provided in brackets above each bar in units of birds per km².

Source: H. T. Harvey & Associates, Schatz Energy Research Center

Power Generation

Power generation potential is proportional to wind speeds at turbine hub height. As wind speed increases, the power output of a turbine increases rapidly until it reaches its rated capacity, at which point the output levels off.

Regional

Because the windscape has been generally quite variable across space and by season, the power generation potential also varies considerably at these scales. The Power Generation Model predicted that a single 12-MW turbine was likely to produce between 8 and 61 gigawatt hours per year (GWh/yr), with higher generation observed further offshore, particularly off Cape Mendocino (Figure 12).

Figure 12: Annual Average Power Generation Potential

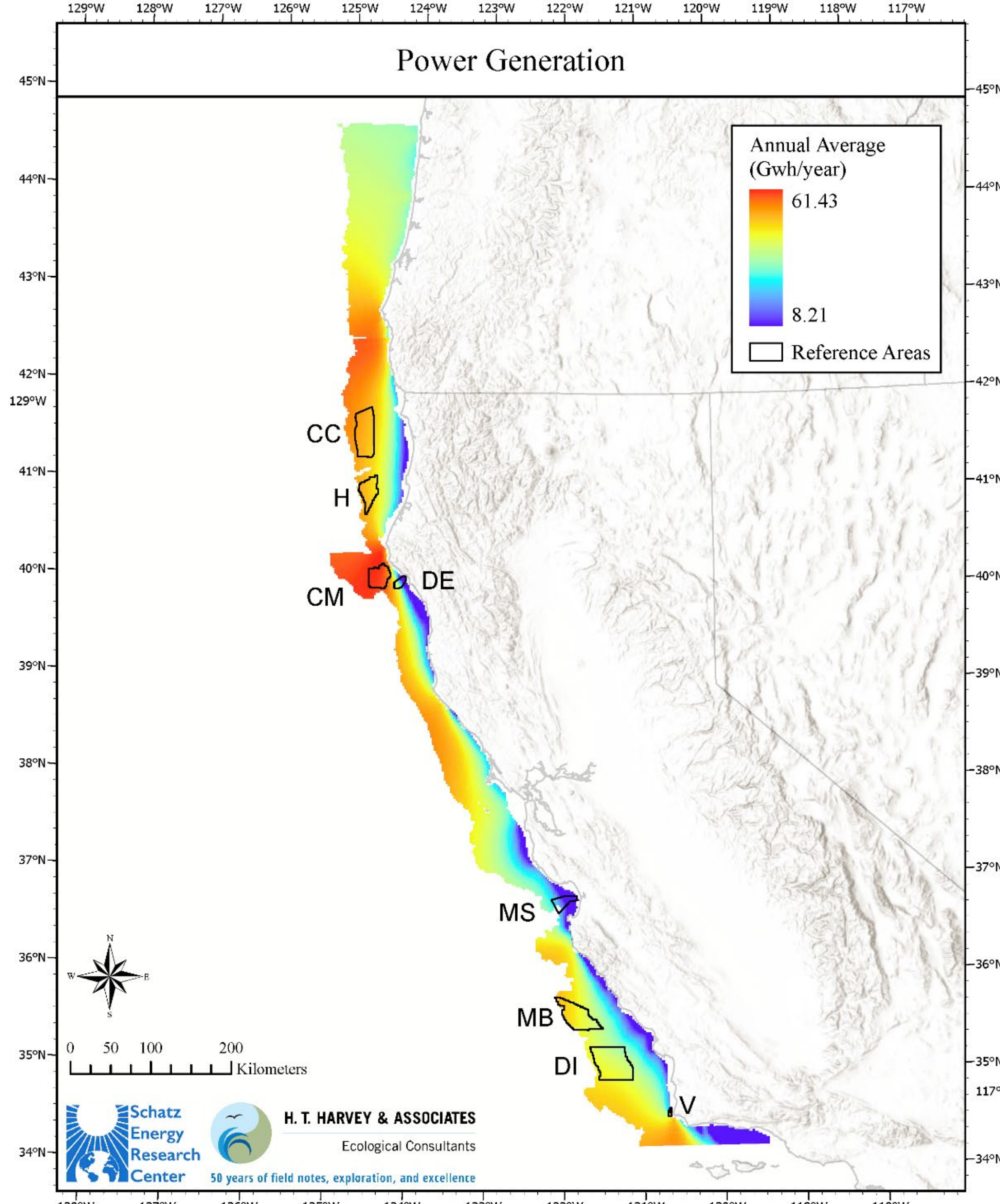

This figure shows estimated annual average power generation (GWh/yr) for a single 12-MW turbine off California and southern Oregon. The color gradient indicates the range of power generation potential, from 8.21 GWh/yr (blue) to 61.43 GWh/yr (red). The black outlines denote reference areas considered in the study, including planned wind facility locations, notional wind facility locations, and two submarine canyon sites, that were selected for their known importance to seabirds in the study area. See Figure 2 for additional study area details, including names of all reference areas.

Source: Schatz Energy Research Center

Reference Areas

A key turbine-performance metric related to power generation potential, capacity factor, is a ratio of how much energy a turbine produces over a time period compared to its maximum possible output over that period. Capacity factor, then, is a ratio between the achieved power generation and the turbine's technically feasible generation. Higher wind speeds and more consistent wind patterns result in higher capacity factors, meaning the turbine is producing closer to its maximum potential. For context, capacity factors around 35 percent are typical for land-based wind power facilities (U.S. Energy Information Administration 2022).

The capacity factors calculated for each scenario in the wind areas included in the study are in excess of 40 percent and some are approaching 60 percent (Cape Mendocino). Both 12-MW and 15-MW turbines showed similar efficiency levels, with capacity factors increasing in areas with higher wind speeds (such as Cape Mendocino; Figure 13). The 600-MW farm configurations consistently demonstrated higher capacity factors due to reduced wake losses compared to full-buildout scenarios. This indicates that these larger configurations are less efficient in harnessing wind energy, leading to lower overall power generation per turbine but higher total power generation because there would be more turbines.

When controlling for variation in facility area and turbine counts, and considering just the windscape, the sites with the most robust wind resources are further offshore and to the north (Cape Mendocino, Humboldt, and Crescent City). The sites with the weakest wind resources were the two seabird reference sites not being considered for wind energy developments (Monterey System and Delgada Canyon). Other sites were intermediate.

In addition to evaluating these scenarios based on capacity factor, they were also compared on a total annual generation basis. This analysis shows the impact of relative size of each wind facility. For any locations where the area can support a buildout larger than 600 MW, full-buildout scenarios always yield greater power generation compared to the 600-MW configuration. Thus, in terms of annual power generation estimates, the number of turbines that can be installed is the most important factor in addition to the windscape (Figure 14).

Figure 13: Capacity Factors for Multi-Turbine Facility Scenarios

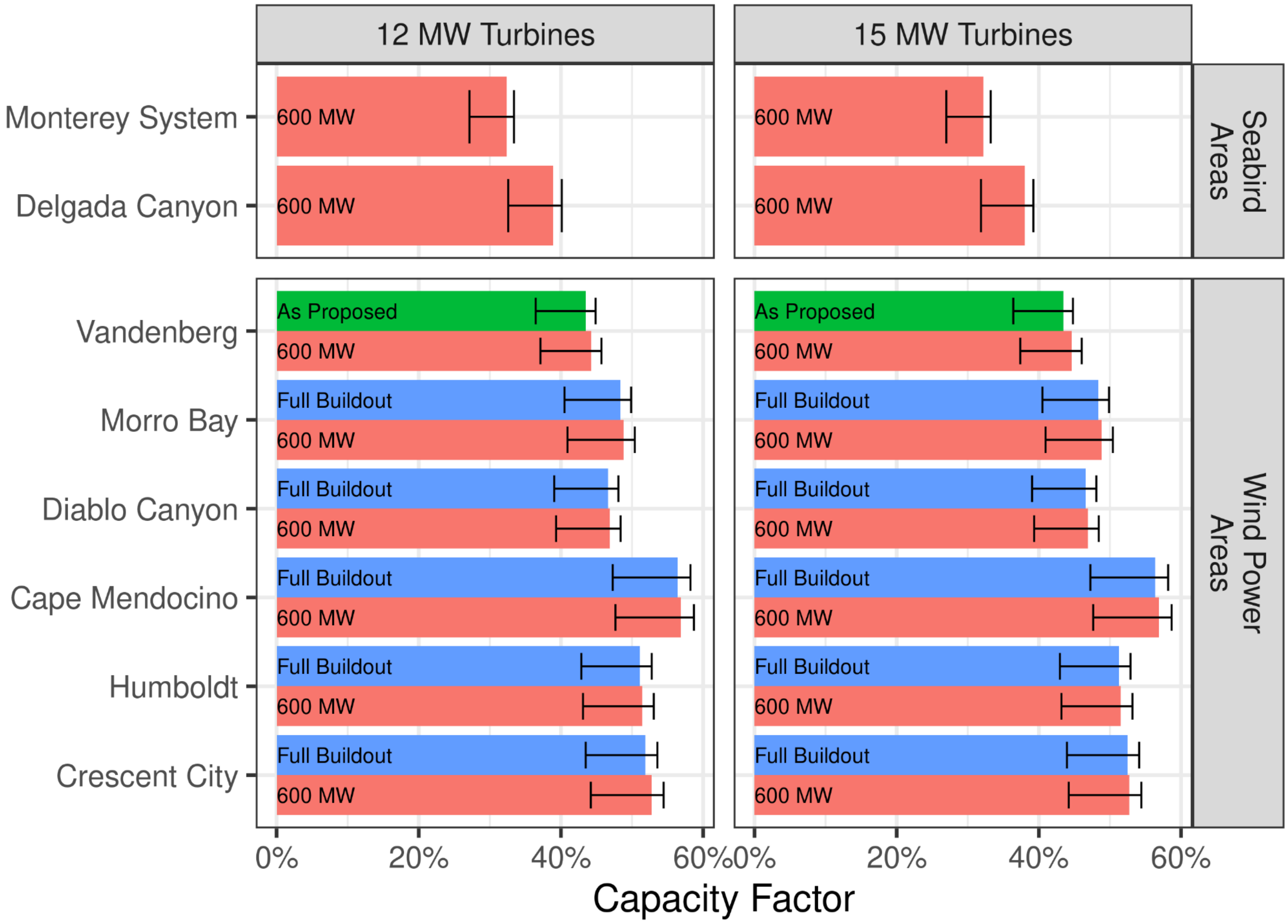

Capacity factors are estimated for various wind facility scenarios, with greater factors representing greater alignment of potential and actual power generation. The error bars reflect a range of uncertainty associated with loss factors. Outcomes represented are colored based on whether they were associated with the 600-MW scenario (pink), the full buildout (blue), and as proposed (green).

Source: Schatz Energy Research Center

Figure 14: Average Annual Power Generation of 12-MW Wind Facility Scenarios

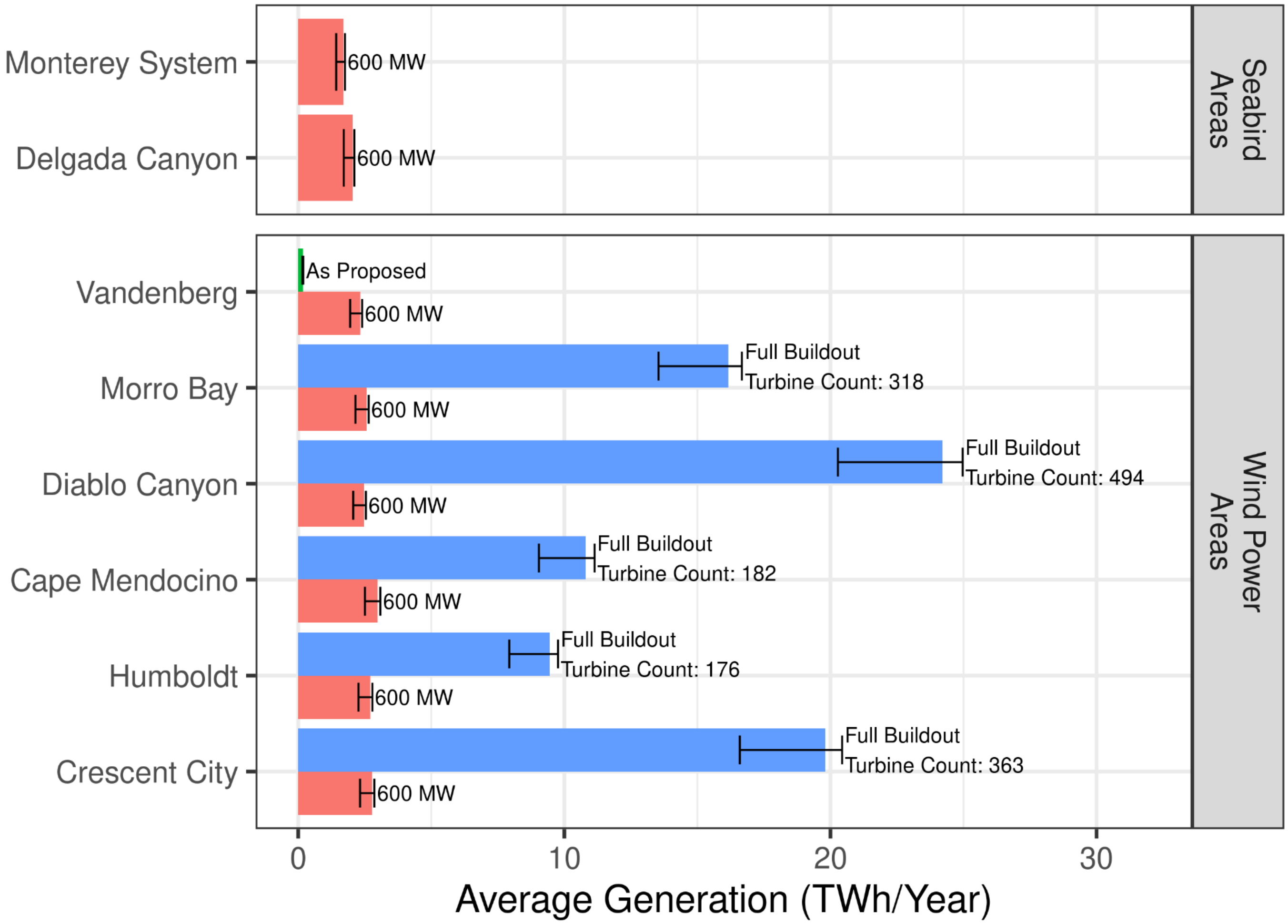

This figure shows average annual power generation, in terawatt-hours per year (TWh/yr), for various wind facility scenarios, including both 600-MW and full-buildout configurations, across multiple locations off the coast of California. Each bar represents the estimated average power generation, with error bars indicating uncertainties associated with loss factors. Outcomes represented are colored based on whether they were associated with the 600-MW scenario (pink), the full buildout (blue), and as proposed (green). Note: 1 TWh/yr equals 1000 GWh/yr.

Source: Schatz Energy Research Center

Multi-objective Optimization

Walkthrough of Framework Predictions

This section provides information about each of the analyses completed for the seabird groups explored in this report. The structure of this section is repeated in the Results section for each seabird group. The walkthrough describes the figures associated with each of the analyses in the order they are presented in the results.

Seabird Density Prediction Maps

Graphical representations of 2D and 3D species-level-density predictions for the 44 seabirds included in the 3D framework aid in interpretation, depicting estimates of the instantaneous densities of the seabird community at all heights ASL and then just at heights exceeding 10 m ASL (examples: Figures 16, 19, 22, and 25).

Interpreting the 2D and 3D Densities: The density estimates, denoted as birds/km², lack a time component. They represent seabird densities expected at any given moment, derived from long-term historical wind speed and seabird data spanning several decades. For example, a predicted density of 35 birds per km² would imply that approximately 35 birds are expected to be present above 10 m ASL within each square km at any given moment based on what was observed, on average, during at-sea surveys from 1980 to 2016.

Additional Details:

- Because the birds above 10 m are a subset of the larger seabird community, the densities presented in the Predicted Above 10 m panel on the left in Figures 16, 19, 22, and 25 will always be less than the densities depicted in the Predicted Total panel on the right.
- Any grid cells lacking a fill color represent areas for which predictions were extremely small (that is, no more than 0.1 birds per km^2or the equivalent of 1 bird every 10 km²). Occurrences of unfilled grid cells are most common in the Predicted Above 10 m map panel.

Benefits:

- Comprehensive Data: The analysis is derived from multi-decadal data, providing a representative range of environmental conditions, including a wide range of extremes.
- Order of Magnitude Expectations: The results offer an understanding of seabird density and distribution overall and at heights more relevant to understanding collision vulnerability, by enhancing preliminary assessments of potential magnitudes of seabird exposure to RSZs.
- Comparative Analysis: The analysis facilitates comparisons across species, sites, and vertical strata, supporting targeted conservation efforts.

Limitations:

- Temporal Sensitivity: The study does not capture the range in magnitude of exposure that could occur from single, point-source events or relatively short periods of anomalous conditions. For example, in a wind event nearing turbine cut-out speeds (25 m/s), over 85 percent of sooty shearwater are estimated to be above 10 m and this, combined with the fact that they are a flocking bird, leads to the potential for short-duration events that contribute greatly to overall vulnerability of individuals being exposed in this population.

- Collision Risk Metrics: The instantaneous density estimates included in the study primarily reflect community vulnerability to collisions but do not directly equate to passage rates or collision rates used in more site-specific collision risk models (CRMs). Actual collision risks at a wind facility are influenced by multiple factors. These include exact passage rates, the composition of seabirds (FGs/species) present at the site, behaviors (such as foraging, transiting, and response to wake turbulence) that might alter an individual's ability to detect and avoid RSZs (that is, the avoidance rate), various physical properties of the turbine being used, and the interactive nature of birds and turbines at a site (such as the angle at which a bird is flying relative to the orientation of the turbine, the exact position of a bird within the RSZ). These factors were not and could not be observed during the at-sea surveys, so true collision risk cannot be meaningfully modeled at this time.

Optimization Framework and Pareto Front Curves

The goal of this analysis was to find an optimal balance between minimizing seabird density above 10 m and maximizing power generation at offshore sites. In Pareto optimization, both variables are typically minimized or maximized. For this analysis, seabird density above 10 m and the inverse of power generation are minimized (effectively maximizing power generation). Thus, the best-performing sites are represented as points nearest the plot origin (values closest to zero).

Interpretation of the Pareto Front: Points along the Pareto front are Pareto-efficient, indicating a potentially attractive tradeoff between minimizing seabird density above 10 m and maximizing power generation. In each Pareto curve, there is a "knee" in the Pareto curve pointed toward the lower left. The steep slope to the left of the knee and the shallow slope to the right of the knee make alternatives near the knee optimal, as these alternatives perform relatively well in both metrics.

Conceptual Example (Figure 15): The black line represents the Pareto front. Points along this line are Pareto-efficient, balancing the two objectives. For example, point A may be Pareto-efficient for minimizing bird density, while point C may be Pareto-efficient for maximizing power generation. Point B represents a balance between both objectives. The knee of the Pareto curve indicates a balance between the two objectives.

Figure 15: Conceptual Pareto Optimization Analysis Curve

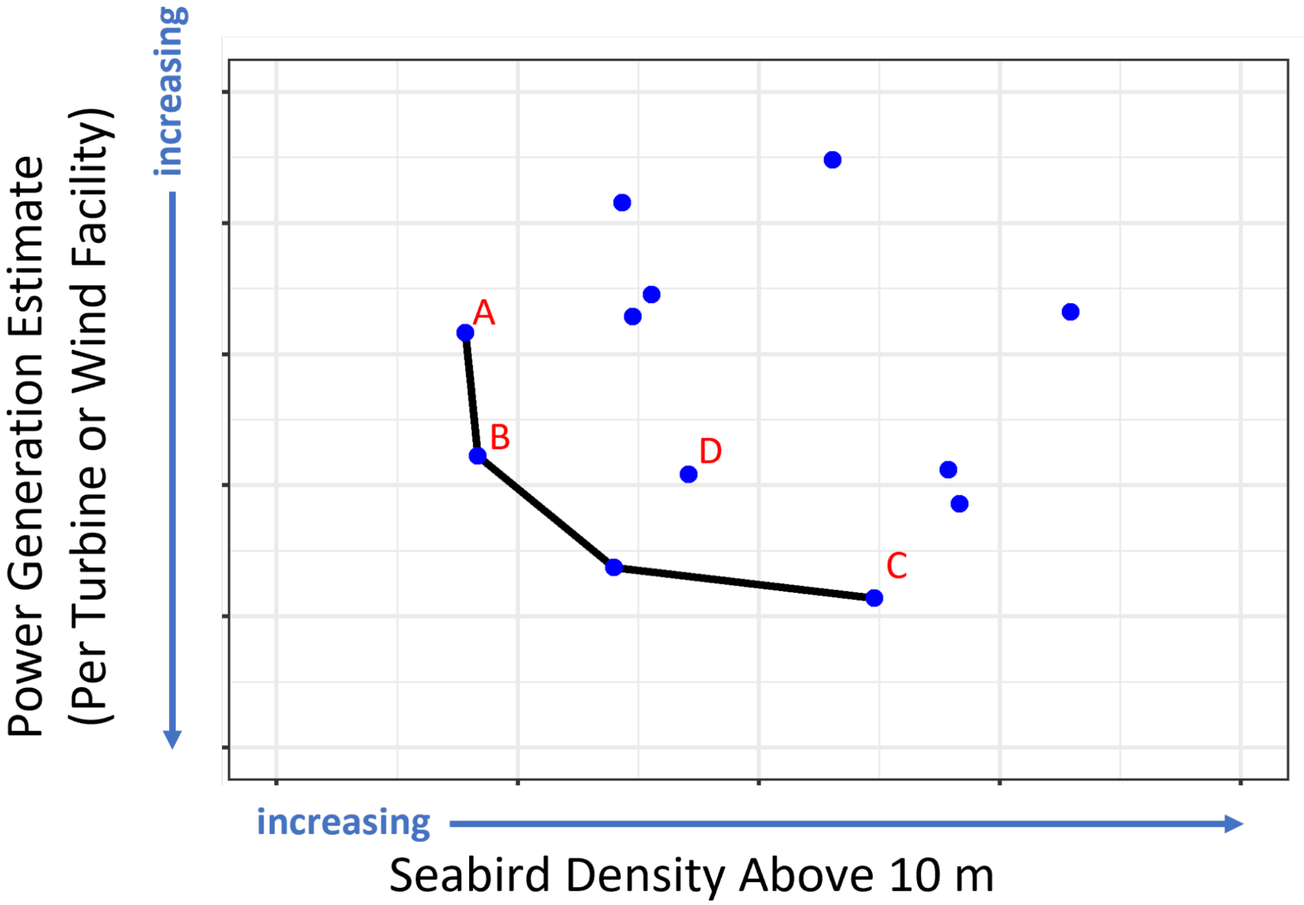

This conceptual example of Pareto optimization analysis illustrates the tradeoffs between two objectives: minimizing seabird density above 10 m and maximizing power generation. The black line represents the Pareto front, with points along this line considered Pareto efficient, meaning no alternatives outperform them in both metrics simultaneously. Points A, B, and C are examples of Pareto-efficient solutions. Point A minimizes seabird density, point C maximizes power generation, and point B offers a balance between the two objectives. Point D, while not Pareto-efficient, still represents a balanced combination of metrics when compared to other alternatives. The knee of the Pareto curve, nearest point B, represents a balance between the two objectives.

Source: Schatz Energy Research Center

Benefits:

- Optimized Decision-making: The analysis provides a clear visualization of the tradeoffs between two critical metrics, helping to identify the most efficient and sustainable sites for wind energy development.
- Balance of Objectives: The results help in identifying sites that offer the best balance between minimizing environmental impact to seabirds and maximizing energy production.
- Comparative Analysis: The analysis facilitates comparison across different sites and configurations, supporting informed decision-making.

Limitations:

- Externalities Not Considered: This analysis considers only bird density above 10 m and the potential for power generation. It does not account for other important factors in siting a wind power facility, such as additional environmental (such as seabird displacement and impacts to marine mammals), social, and economic issues.
- Feasibility: Areas that appear Pareto-efficient in this analysis may not be feasible for floating OSW development due to other technical or logistical constraints.
- Complexity for Non-experts: While the graphical representation simplifies these data, the concept of Pareto efficiency and the interpretation of the tradeoffs might still be complex for interested parties without a technical background in optimization analysis.

Single Turbine Analysis

To get a sense of the relative co-benefits across the entire study area, this section presents results of placing a single wind turbine in each cell of thousands of regularly spaced locations across the study area. Each of these single turbine scenarios is then treated as an alternative in a Pareto analysis. The figures include a map showing how close each cell is to the Pareto front and a plot of Pareto optimization analysis curves. This analysis compares the typical annual power generation (GWh/yr) for a single 12-MW turbine (shown in reverse order) with the average bird density above 10 m (birds/km^2). The black line represents the Pareto front, with points colored to show their distance from the front.

The lower panel of the figure focuses on the closest 20 percent of cells to the Pareto front. It uses a simple (k-means) grouping analysis to show how different locations can be grouped, based on their balance between power generation and bird vulnerability. The organization of the lower panel mirrors the top figure, with the right graphic showing these alternatives in solution space and the left showing them on the map (examples: Figures 17, 20, 23, and 26).

Wind Facility Scenario Analysis

The team explored 32 turbine scenarios: 16 scenarios with 12-MW turbines and 16 with 15-MW turbines. However, 12-MW and 15-MW scenarios showed similar annual power generation for a given rated capacity (Power Generation results section). Additionally, the seabird vulnerability metric used in this study was estimated on a per-turbine basis, making it difficult to meaningfully compare 12-MW to 15-MW turbines. Therefore, the optimization results presented here focus solely on the 12-MW turbines. These consist of 8 600-MW scenarios and 8 full-buildout scenarios; however, results are not shown for the full buildout scenarios at the smaller reference areas (Delgada Canyon, Monterey System, and Vandenberg).

Pareto curves were presented in two ways:

1. Left Panel: Trades off total vulnerability and energy generation metrics. This approach accounts for different buildout levels in various areas but often concludes that larger wind facilities pose a greater threat to birds than smaller facilities.
2. Right Panel: Uses per-turbine metrics, which are better for directly comparing the estimated seabird densities in two locations.

Curves presented in this section use 1- or 2-letter abbreviations to relate points (in solution space) to the reference areas. The location of all power generation reference areas, along with each of their 1- or 2-letter acronyms, are provided in graphical format.

Additionally, the very small facility scenario (Vandenberg) is excluded from the analysis that considers full buildout scenarios. With only four proposed turbines, this scenario is an outlier, providing far less total generation and far less estimated seabird vulnerability because it would be a small project (examples: Figures 18, 21, 24, and 27).

Optimization Results for All Seabirds

Density Predictions

The first grouping explored includes all 44 seabird species, showing vulnerability of the entire seabird community. Figure 16 provides a comprehensive visualization of seabird density predictions for all elevations (2D) as well as specifically above 10 m (3D) . Broadly, densities drop considerably above 10 m, with about 8 percent of the seabird community predicted to be above 10 m. Additionally, seabird densities are expected to be greatest near the coast, decreasing with increasing distance from the shore, and to the south, decreasing moving north.

Total Density (All Elevations): The left panel shows the predicted total seabird density (birds/km²) across the study area. The overall mean density for all elevations is 36 birds/km², with a maximum density of 127 birds/km² observed in certain coastal hotspots. There is a clear gradient in seabird density from the coast to beyond the shelf-break, with greater densities closer to shore (more than 100 birds/km²) and the greatest densities predicted in association with the Monterey System. Medium-density areas (10-50 birds/km²) extend further offshore but remain relatively close to the coastline.

Density Above 10 meters: The right panel focuses on seabird density predictions at elevations above 10 m. Compared to the total density, the densities expected above 10 m are significantly lower, reflecting the smaller proportion of seabirds flying at these heights. The reduction in density at greater altitudes is consistently about 92 percent across the study area, indicating that seabirds are less frequently found at these heights. The overall mean density above 10 m is 2.845 birds/km², with a maximum density of 17.821 birds/km² in offshore areas. High-density areas above 10 m (more than 10 birds/km²) generally mirrored what was expected with total density.

Figure 16: Density Predictions for All Seabirds

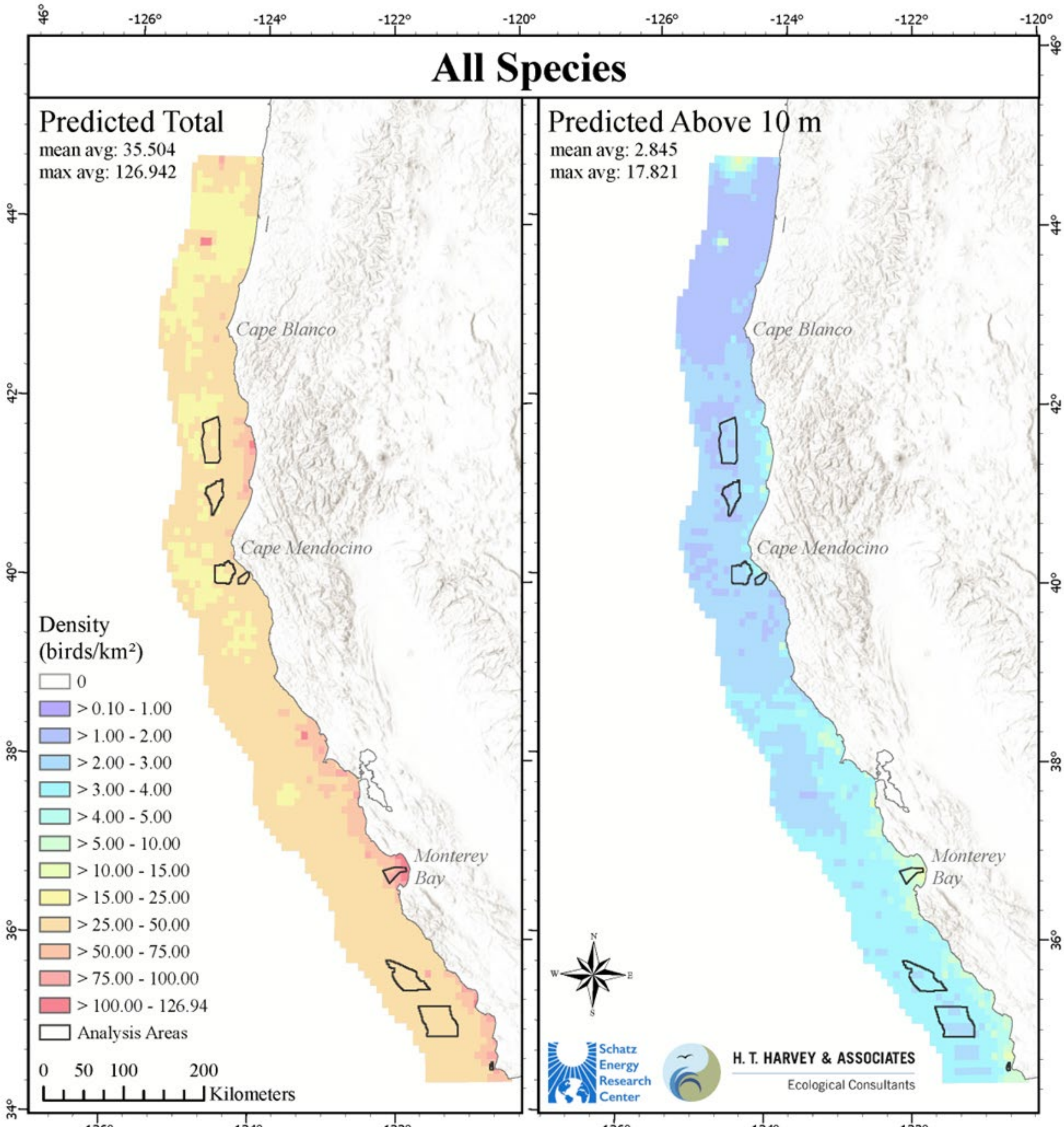

This figure illustrates how seabird density predictions change when considering all birds (left) versus only those birds flying above 10 m (right). The figure also highlights how seabird densities at rotor swept height vary across space. Black outlines denote reference areas (see Figure 2) highlighted by this study; these include planned wind facility locations, notional wind facility locations, and submarine canyon areas known to host a diversity and density of seabirds. All values presented here have units of birds per km².

Source: H. T. Harvey & Associates, Schatz Energy Research Center

Single Turbine Analysis Outcomes

Figure 17 provides a comprehensive visualization of how different locations balance the tradeoffs between seabird vulnerability and wind energy generation. Alternative sites on the Pareto front can achieve the full range of power generation with bird densities below 2.0 birds/km². In locations where vulnerability is maximized, bird densities were predicted to be on the order of 20 birds/km². Following are key takeaways.

Spatial Distribution (Top: Right): Areas far from the coast, starting around Cape Mendocino and northward, are nearer to the Pareto front, indicating that is the region having an attractive tradeoff between seabird densities above 10 m and power generation. Areas in the south and near to shore fall furthest from the Pareto front, as these southern, nearshore areas tend to have relatively numerous birds and relatively low power generation potential.

Grouping of Nearest 20 Percent of Cells (Bottom: Right): This panel zooms in on the 20 percent of cells closest to the Pareto front and colors them based on relative weighting of objectives. This graphic shows that areas off Cape Mendocino are optimal for power generation, whereas areas to the far north of the study area are optimal from a seabird vulnerability perspective. Areas offshore of the California-Oregon border show a good balance of objectives.

Figure 17: Pareto Optimality Analysis for All Seabirds

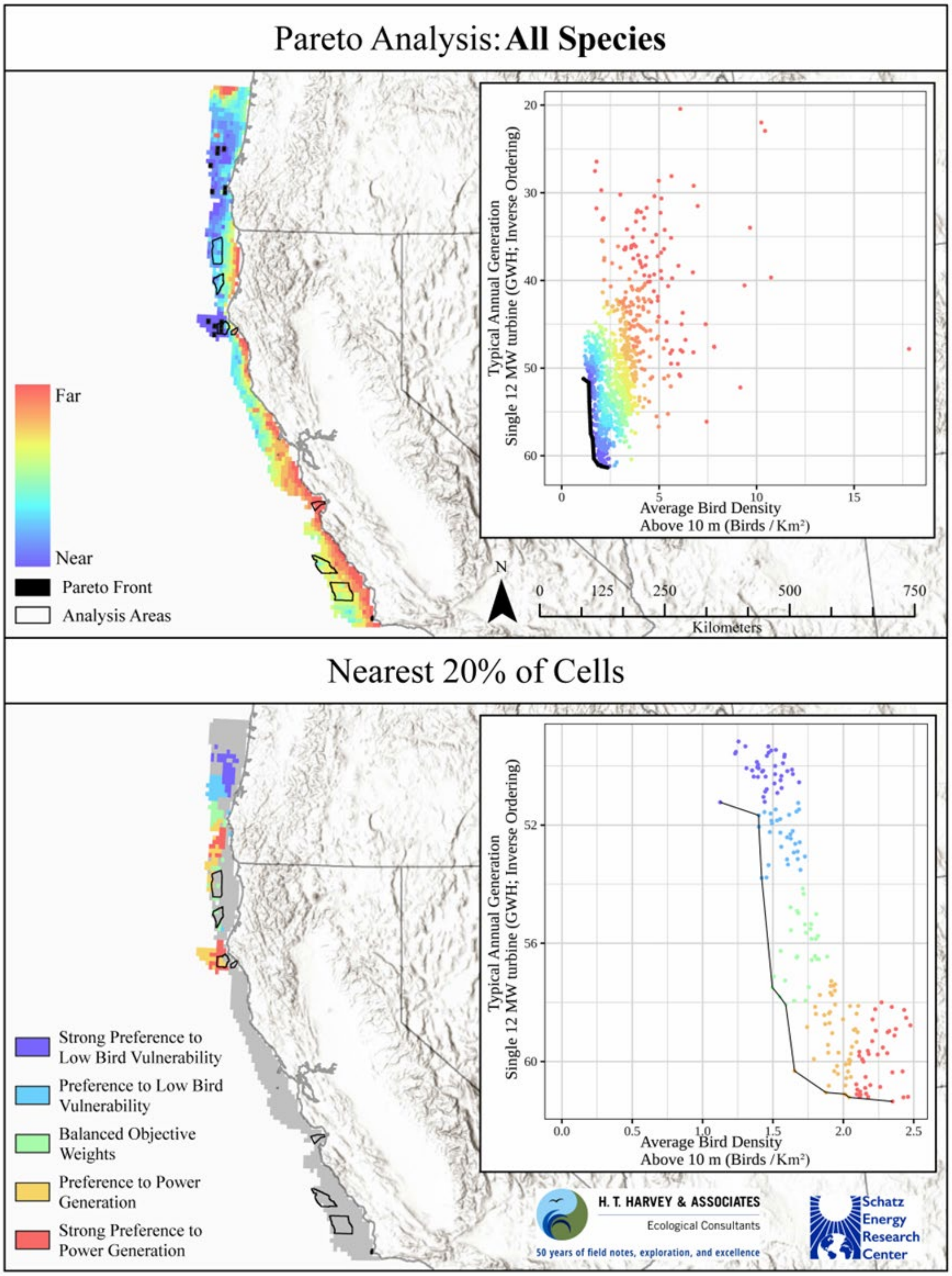

This figure shows the Pareto optimality analysis for all seabird species included in the Optimization Framework, highlighting the tradeoffs between seabird density above 10 m and power generation for a single 12-MW turbine. The top panel shows the spatial distribution of the Pareto front, with colors indicating the distance of each cell from this frontier. The inset graph within the top panel presents the Pareto front in solution space, with each point representing a potential turbine location and colored by its distance from the Pareto front. The bottom panel highlights the top 20 percent of cells closest to the Pareto front, categorizing sites based on their tendency to prioritize either low bird vulnerability, power generation, or a balanced approach.

Source: Schatz Energy Research Center, H. T. Harvey & Associates

Pareto Front (Left/Inset Graphs): The inset graphs illustrate how different wind energy sites balance the goals of power generation and seabird density (above 10 m), with each point representing a potential site and how well it meets these objectives. The top inset graphic shows all potential sites, color-coded to indicate their distance from the Pareto Front. The bottom inset graphic focuses on the top 20 percent of objectives, colored by objective weighting preference. The shape of this Pareto curve shows that these two objectives are largely not in conflict. Alternatives that span the full range of power generation are available at less than 2.5 birds per km^2, while maximum estimates of bird density (above 10 m) exceed 15 birds per km^2The noticeable knee in the Pareto curve, pointing to the lower left, highlights the most balanced sites. These sites perform well in both power generation and minimal impact on seabirds.

Wind Facility Analysis Outcomes

When total facility metrics were evaluated (Figure 18, left panel), a key pattern that emerged was that locations capable of supporting a larger number of turbines exhibited greater total power generation and increased bird densities. This illustrates the inherent tradeoff between scaling up wind energy capacity and the associated risks to seabirds. As facilities increase in size, the cumulative impact on seabird populations is likely to increase, though not likely in a linear fashion.

When considering per-turbine metrics (Figure 18, right panel):

- The notional Cape Mendocino reference area has the highest power generation per turbine, highlighting its robust wind resources.
- Only the notional Cape Mendocino and Crescent City reference areas fall on the Pareto front, due to their relatively large potential to generate energy on a per-turbine basis and relatively low bird densities, indicating favorable wind conditions and lowest collision vulnerability at these locations. The Humboldt WEA is very near, but not on, the Pareto front.
- Other sites have higher average bird densities per turbine compared to locations on the Pareto front and lower potential for power generation.
- The distribution of sites along the Pareto front shows a clear separation between those with greater potential for renewable generation and those that are better for seabird protection, highlighting the importance of balancing these two metrics in site selection.

This highlights the importance of evaluating total and per-turbine metrics to understand the potential impacts of wind energy facilities on seabird populations. Until there are further studies exploring attraction and avoidance behaviors, it is not known how much the size of a facility (in terms of turbine count) alters marginal impacts for additional turbines (that is, the additional impact for adding a single turbine to a large facility versus a small facility).

Figure 18: Pareto Analysis for Reference Areas Based on All Seabirds in the Framework

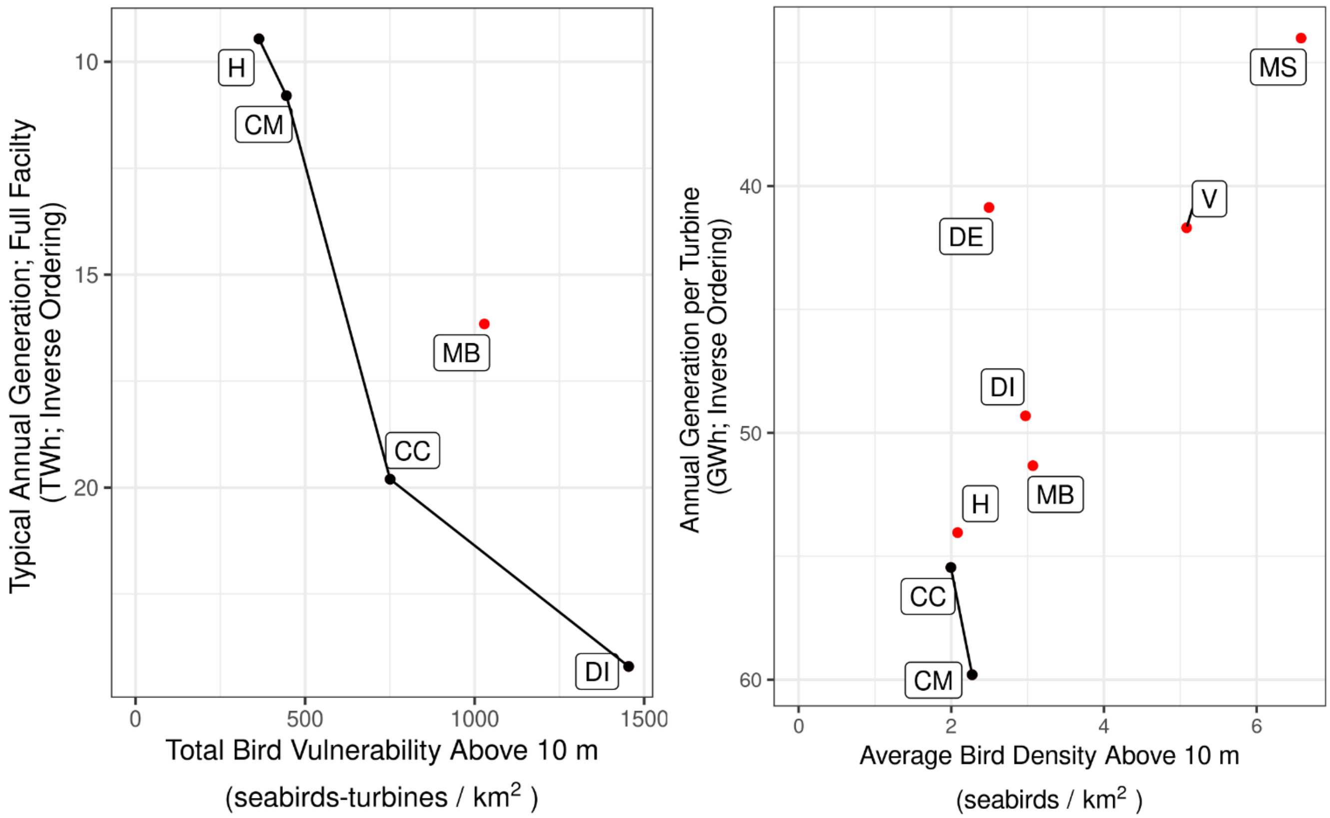

Pareto optimality analysis curves for all seabirds included in the Optimization Framework illustrate the tradeoffs between seabird density above 10 m and power generation for different wind facility scenarios simulated at the reference areas. The left panel compares total bird vulnerability (sum of birds per turbine per km²) with typical annual generation (TWh/yr) for the full facility, while the right panel compares average bird density (birds/km²) above 10 m with annual generation per turbine (GWh/yr). Black points on the Pareto front indicate scenarios that offer the best tradeoffs between minimizing bird density and maximizing power generation. A total of eight sites were analyzed: Crescent City (CC), Cape Mendocino (CM), Delgada Canyon (DE), Diablo Canyon (DI), Humboldt (H), Morro Bay (MB), Monterey System (MS), and Vandenberg (V).

Source: Schatz Energy Research Center

Group-specific Outcomes

This section presents detailed case studies focusing on specific seabird groups to provide a nuanced understanding of the tradeoffs between seabird vulnerability and wind energy generation. By including rare and common species, this project aims to provide a comprehensive assessment that minimizes the vulnerability of special-status species while also considering the potential widespread ecological impacts.

Abundant Species off California

While the most common species are not afforded the same level of legal protection as those that are federally and state listed as threatened or endangered, they do receive protection under the federal Migratory Bird Treaty Act and (in state waters) the California Department of

Fish and Game Code. The species most likely to encounter RSZs are those that are most dense above 10 m ASL. For this, the results for the two most abundant seabird groups expected above 10 m ASL are presented: 1) the most abundant single species in the area, the dynamically soaring sooty shearwater, and 2) the assemblage of gull species. These two seabird taxa account for 80 percent of the seabird community expected above 10 m ASL. The remaining 20 percent of individuals consisted of a broad diversity of FGs and species.

Sooty Shearwater

A single species, the sooty shearwater, accounts for 19.3 percent of all seabirds predicted to be above 10 m. Additionally, this species accounts for almost 97 percent of all dynamically soaring species expected above 10 m in the study area. Thus, mapping the sooty shearwater also provides a sense of the overall vulnerability pattern expected for all dynamic soaring species. The densities of sooty shearwater are an order of magnitude greater than other dynamically soaring seabirds in the region (Figure 19).

Density Predictions

Total Density (All Elevations): The left panel shows the predicted total density of sooty shearwaters across the study area. The overall mean density for all elevations is 9.7 birds/km², with a maximum density of 95.8 birds/km² observed in specific coastal regions. Sooty shearwaters are relatively abundant across the entire region, with densities predicted to be greatest in association with the Monterey System.

Density Above 10 Meters: The right panel focuses on sooty shearwater density predictions at elevations above 10 m. Compared to the total density, the mean densities expected above 10 m are approximately 92 percent lower than the total mean density. Thus, the pattern of reduced densities with increasing flight height is apparent for sooty shearwaters as well. Given average wind conditions across the study area, 5.7 percent of the sooty shearwater population is expected to be at 10 m or greater across the study area (Appendix A). This percentage is likely to vary considerably in response to real-time variation in wind conditions across the study area. This variation is due to the propensity for sooty shearwaters (and other dynamic soaring seabirds) to be relatively unlikely to fly above 10 m ASL at slow wind speeds, and relatively likely to fly above 10 m ASL at fast (greater than 15–20 m/s) wind speeds. When winds are non-existent, or very low, most shearwaters remain on the water.

Figure 19: Density Predictions for Sooty Shearwater

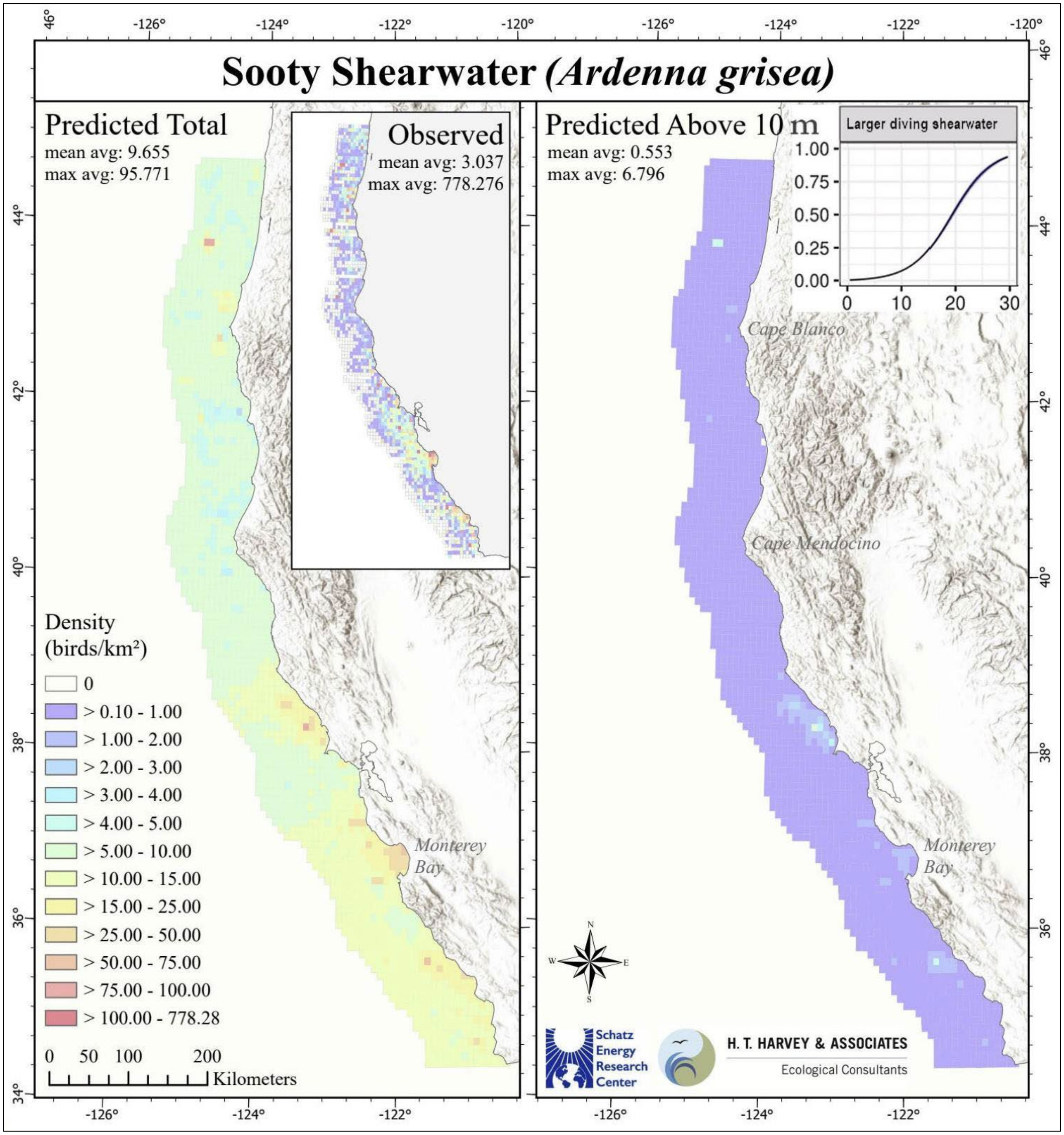

This figure illustrates how sooty shearwater density predictions change when all birds (left) are considered versus only those birds flying above 10 m (right). The figure also highlights how shearwater densities at rotor swept height vary across space. All values presented here have units of birds per km².

Source: H. T. Harvey & Associates, Schatz Energy Research Center

Single Turbine Analysis Outcomes

Figure 20 provides a comprehensive visualization of how different locations balance the tradeoffs between sooty shearwater collision vulnerability and wind energy generation). Alternative sites can achieve the full range of power generation with shearwater densities below 0.4 birds/km². In scenarios with the greatest vulnerability, shearwater densities were predicted to be on the order of 6 birds/km². This Pareto curve has a sharp knee that would indicate that seabird and power generation objectives are largely not in conflict.

The general patterns observed are similar to those in the All Species map (Figure 17): (1) areas far from the coast, starting around Cape Mendocino and northward, are closer to the Pareto front, (2) areas off Cape Mendocino are optimal for power generation, (3) areas to the far north have decreased seabird vulnerability, and (4) areas offshore of the California-Oregon border show a good balance of objectives. A side-by-side graphic comparison of the All Species (Figure 17) and the sooty shearwater (Figure 20) reveals that sooty shearwaters exhibit distinct concentration patterns influencing the classification of sites on the front and meeting balanced weight objectives. Specifically, sites far to the north and nearshore sites north of Cape Mendocino appear most optimal from a perspective of minimizing vulnerability to sooty shearwater, whereas sites most optimal from the broader community perspective were more centered off Cape Blanco in Southern Oregon.

Figure 20: Pareto Optimality Outcomes for Sooty Shearwater

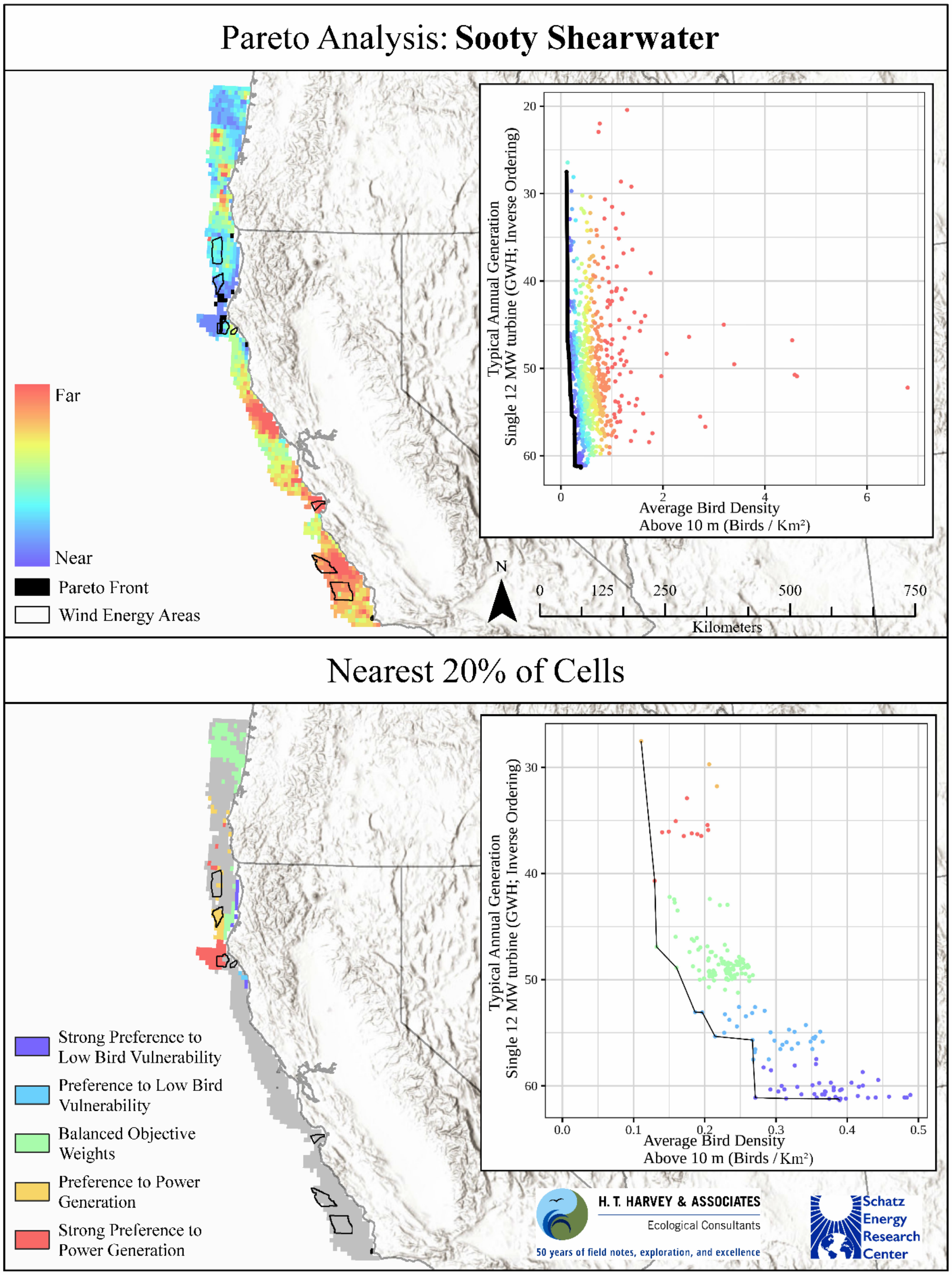

The Pareto optimality analysis for sooty shearwaters highlights the tradeoffs between density above 10 m and power generation for a single 12-MW turbine. The top panel shows the spatial distribution of the Pareto front, with colors indicating the distance of each cell from this frontier. The inset graph within the top panel presents the Pareto front in solution space, with each point representing a potential turbine location and colored by its distance from the Pareto front. The bottom panel highlights the top 20 percent of cells closest to the Pareto front, categorizing sites based on their tendency to prioritize either low bird vulnerability, power generation, or a balanced approach.

Source: Schatz Energy Research Center, H. T. Harvey & Associates

Wind Facility Analysis Outcomes

When evaluating total facility metrics (Figure 21, left panel), the positioning of all sites relative to the Pareto front mirrored that of the All Species outcome (Figure 18), with all sites except the Morro Bay WEA falling on the Pareto Front. This is due to the notional Cape Mendocino and Crescent City areas outperforming the Morro Bay WEA in both power generation and seabird metrics.

When considering per-turbine metrics (right panel), the sites falling on the Pareto front are the Humboldt WEA and the notional Cape Mendocino area. These two sites were predicted to outperform all other sites in power generation and seabird metrics simultaneously, with the exception of Crescent City showing a better wind resource than Humboldt. In the All Species aggregate (Figure 18), the outcome was very similar; however, Crescent City was on the Pareto front and Humboldt was not.

Figure 21: Pareto Analysis for Reference Areas Based on Sooty Shearwater

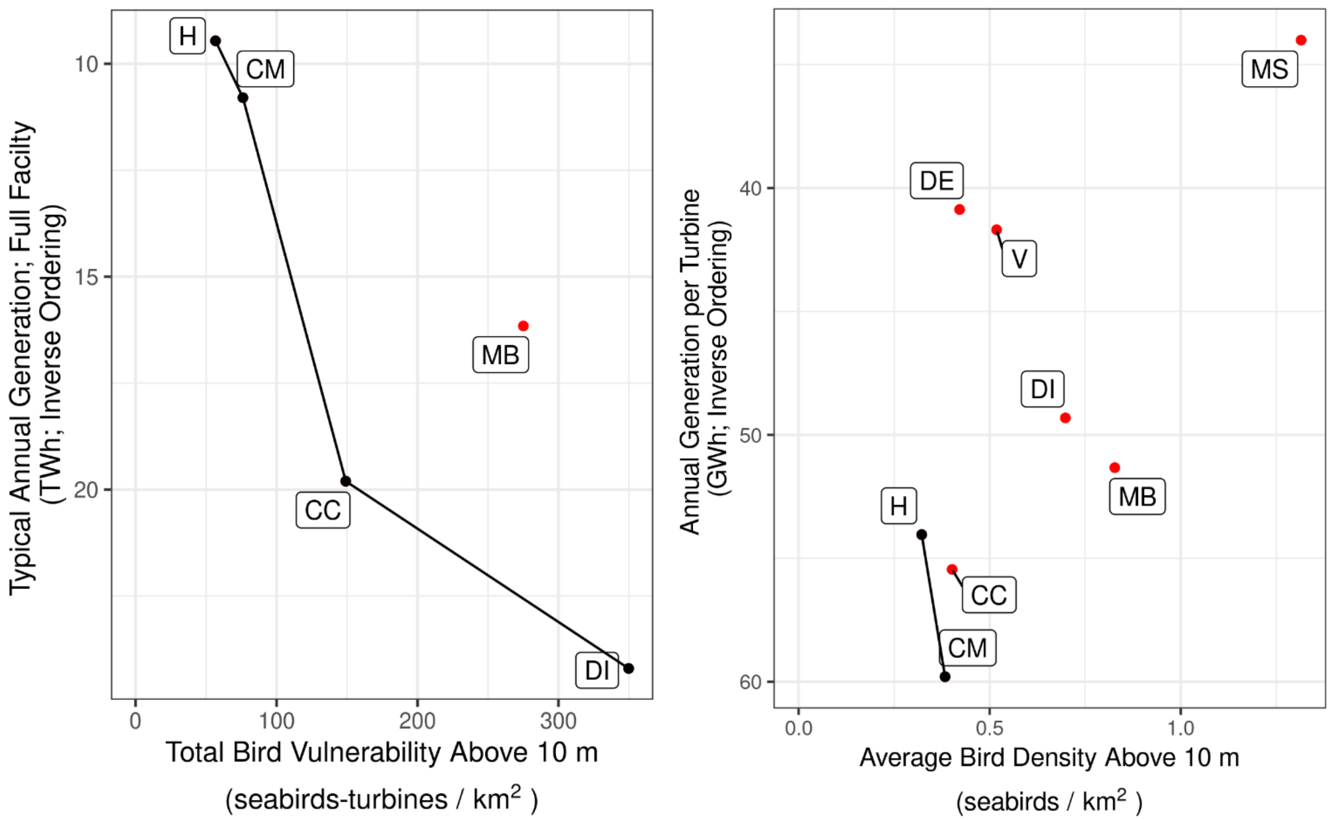

Pareto optimality analysis curves for sooty shearwaters illustrate the tradeoffs between density above 10 m and power generation for different wind facility scenarios simulated at the reference areas. The left panel compares total bird vulnerability (sum of birds per turbine per km²) with typical annual generation (TWh/yr) for the full facility, while the right panel compares average bird density (birds/km²) above 10 m with annual generation per turbine (GWh/yr). Black points on the Pareto front indicate scenarios that offer the best tradeoffs between minimizing bird density and maximizing power generation. A total of eight sites were included: Crescent City (CC), Cape Mendocino (CM), Delgada Canyon (DE), Diablo Canyon (DI), Humboldt (H), Morro Bay (MB), Monterey System (MS), and Vandenberg (V).

Source: Schatz Energy Research Center

Gulls

The gulls (Family Laridae) group includes nine species of small, medium, and large gulls regularly present off California. These nine species, listed from most to least abundant, are: California gull, western gull, black-legged kittiwake, herring gull, Bonaparte's gull, glaucous-winged gull, Heermann's gull, Sabine's gull, and short-billed gull (see Appendix A for species-specific counts and prediction details). Mapping gulls provides a sense of the overall risk pattern expected due to their densities accounting for more than half of the birds expected at RSZ-height (Figure 22). One potential complication to keep in mind is that the two highly migratory Bonaparte's and Sabine's gulls occur in large numbers during just a short migration period as they pass through the area, mostly along the shelf break. Given the nature of this study, capturing observations of temporally transient species is challenging. Thus, their density likely underestimates their actual vulnerability to OSW development and might require more targeted surveys.

Density Predictions

Total Density (All Elevations): The left panel shows the predicted total density of gulls across the study area. The overall mean density for all elevations is 5.045 birds/km², with a maximum density of 48.213 birds/km² observed in specific coastal regions. Gulls are relatively abundant across the whole region, with the main density gradient showing that they have been, and are predicted to be, slightly more concentrated coastally and to the south.

Density Above 10 Meters: The right panel focuses on gull density predictions at elevations above 10 m. Compared to the total density, the mean densities expected above 10 m are approximately 65 percent lower than the total mean density. Thus, the pattern of reduced densities with increasing altitude was apparent for gulls as well; given average wind conditions across the study area and varying slightly from species to species, about 35 percent of the gull population is expected to be at 10 m or greater across the study area (Appendix A). This percentage likely would be relatively stable, even in years with wind conditions that are anomalously slow or fast, due to gulls being relatively likely to fly above 10 m ASL at the range of wind speeds from 0 to 30 m/s.

Figure 22: Density Predictions for Small, Medium, and Large Gulls

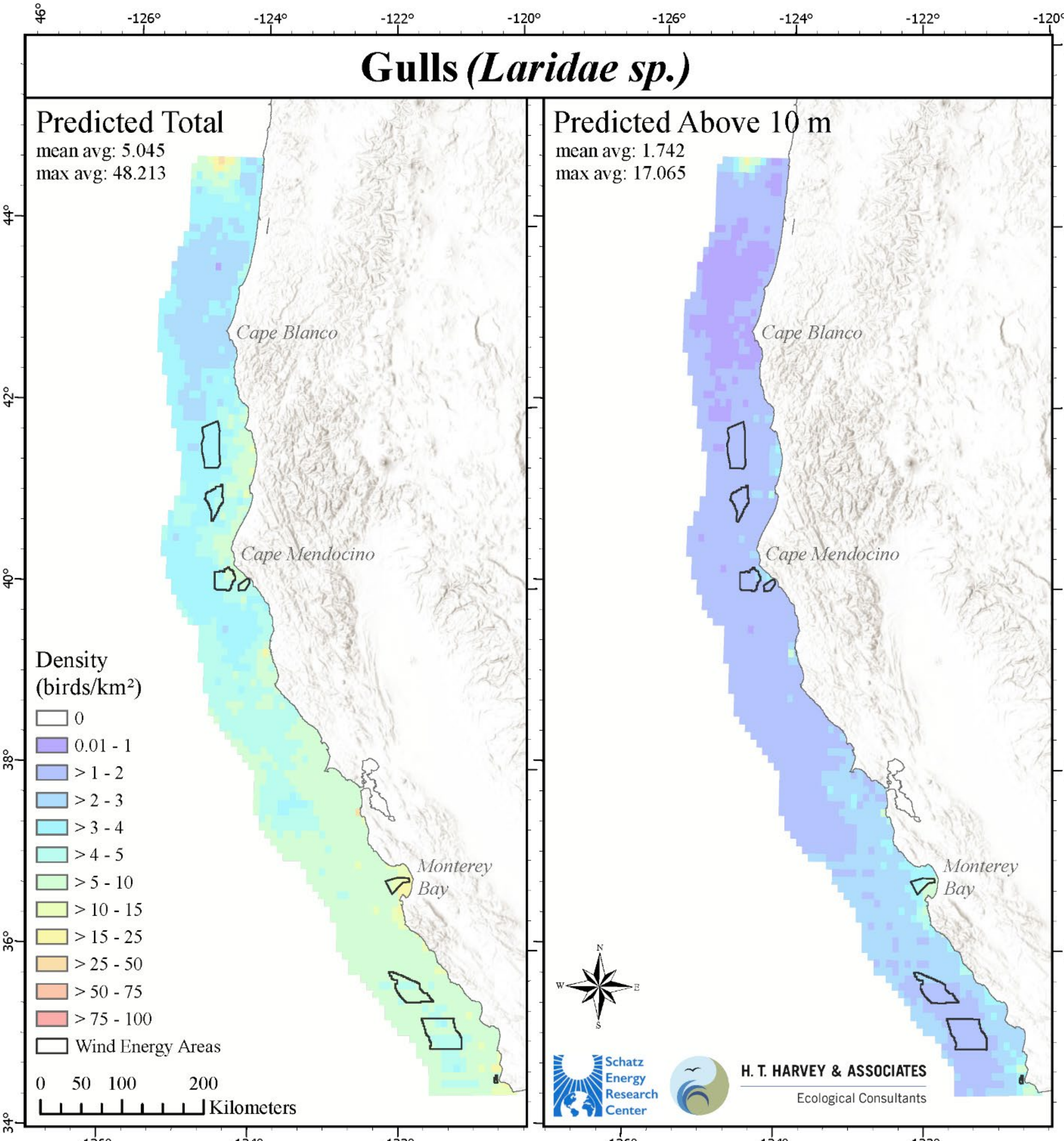

This figure illustrates how gull density predictions change when all birds (left) are considered versus only those birds flying above 10 m (right). The figure also highlights how gull densities at rotor swept height vary across space. Black outlines denote references areas (see Figure 2) highlighted by this study, which include planned wind facility locations, notional wind facility locations, and submarine canyon areas known to host a diversity and density of seabirds. All values presented here have units of birds per km².

Source: H. T. Harvey & Associates, Schatz Energy Research Center

Single Turbine Analysis Outcomes

Figure 23 provides a comprehensive visualization of how different locations balance the tradeoffs between gull collision vulnerability and wind energy generation. For gulls, alternative sites on the Pareto front can achieve the full range of power generation with bird densities below 1.5 birds/km². This Pareto curve has a sharp knee that would indicate that seabird and power generation objectives are largely not in conflict.

The general patterns observed are similar to those in the All Species map (Figure 17): (1) areas far from the coast, starting around Cape Mendocino and northward, are closer to the Pareto front, (2) areas off Cape Mendocino are most optimal for power generation, (3) areas to the far north have lower gull vulnerability, and (4) areas offshore of the California-Oregon border show a good balance of objectives. A side-by-side comparison of the All Species and gull graphics reveals that gulls exhibit concentration patterns that result in nearly identical placement of sites on the front and meeting balanced weight objectives.

Figure 23: Pareto Optimality Outcomes for Gulls

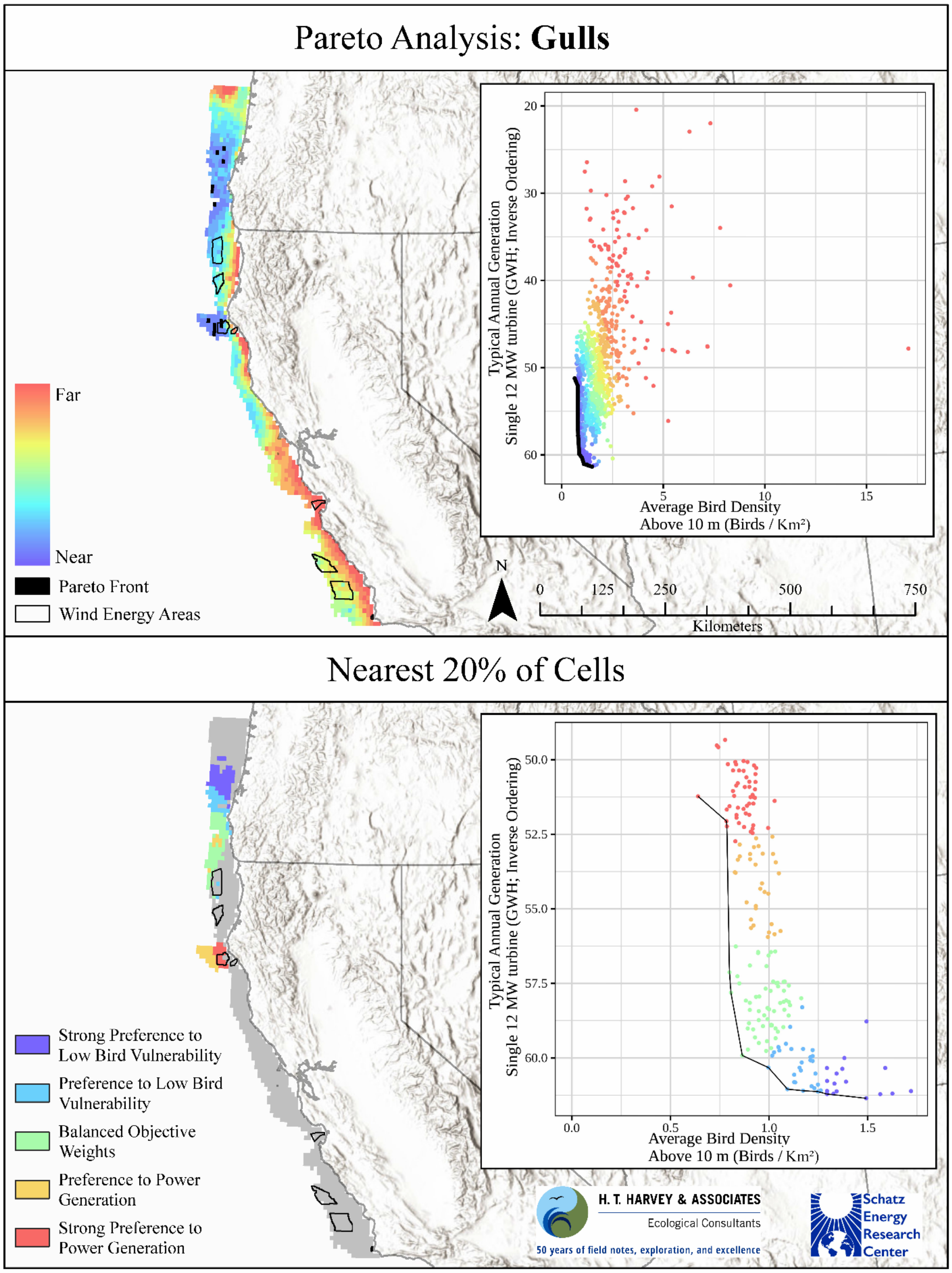

This figure illustrates the Pareto optimality analysis for gulls, highlighting the tradeoffs between density above 10 m and power generation for a single 12-MW turbine. The top panel shows the spatial distribution of the Pareto front, with colors indicating the distance of each cell from this frontier. The inset graph within the top panel presents the Pareto front in solution space, with each point representing a potential turbine location and colored by its distance from the Pareto front. The bottom panel highlights the top 20 percent of cells closest to the Pareto front, categorizing sites based on their tendency to prioritize either low bird vulnerability, power generation, or a balanced approach.

Source: Schatz Energy Research Center, H. T. Harvey & Associates

Wind Facility Analysis Outcomes

Like the Single Turbine Analysis Outcomes, the outcomes for the aggregate community of gulls (Figure 24) are very similar to that of the All Species scenario (Figure 18); site positions relative to each other and relative to the Pareto front match. When evaluating total facility metrics (left panel), in all cases, it is important to note that locations capable of supporting a larger number of turbines exhibited greater total power generation as well as increased bird vulnerabilities. When considering per-turbine metrics (right panel), only the notional Crescent City and Cape Mendocino areas fall on the Pareto front, with the Humboldt WEA being near the front but outperformed in both seabird and power generation metrics by Crescent City.

Figure 24: Pareto Analysis for Reference Areas Based on Gulls

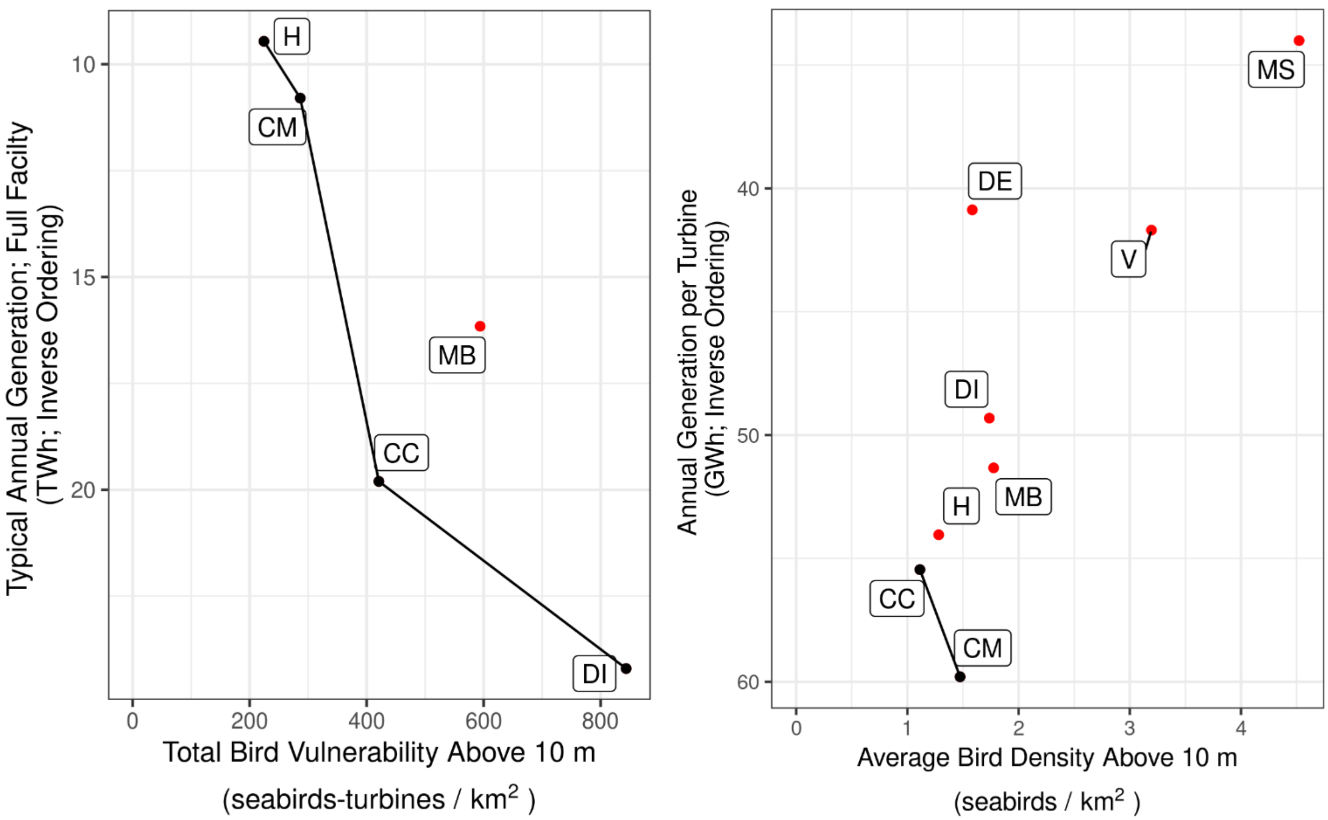

The Pareto optimality analysis curves for gulls illustrate the tradeoffs between density above 10 m and power generation for different wind facility scenarios simulated at the reference areas. The left panel compares total bird vulnerability (sum of birds per turbine per km²) with typical annual generation (TWh/yr) for the full facility, while the right panel compares average bird density (birds/km²) above 10 m with annual generation per turbine (GWh/yr). Black points on the Pareto front indicate scenarios that offer the best tradeoffs between minimizing bird density and maximizing power generation. A total of eight sites were included: Crescent City (CC), Cape Mendocino (CM), Delgada Canyon (DE), Diablo Canyon (DI), Humboldt (H), Morro Bay (MB), Monterey System (MS), and Vandenberg (V).

Source: Schatz Energy Research Center

Federal and State ESA-listed Species

Results for ESA-listed species are intended to highlight broad patterns of collision vulnerability for species that are of increased conservation concern due to compromised population viability. These species receive elevated legal protection due to their ESA status (Figure 25). However, as noted in the methods, the only ESA-listed species with observations sufficient for inclusion in the 3D Framework were from a single FG, small alcids: marbled, Scripps's, Guadalupe, and/or Xantus's murrelet. Thus, the map presented for this aggregate of birds is only depicting the extremely low (near 0) likelihood that murrelets will be present at or above 10 m anywhere across the entire study area. Although Hawaiian petrel and short-tailed albatross are also federally listed, observations were insufficient to include these species in this initial application of the 3D Collision Vulnerability Framework. Only State and Federal listed species are included here, not State Species of Special Concern nor any other official list of species of concern (such as the International Union for Conservation of Nature Red List).

Density Predictions

Total Density (All Elevations): The left panel shows the predicted total density of Federal and/or State ESA-listed species (murrelets) across the study area. The overall mean density for all elevations is 0.056 birds/km² (about 0.16 percent of the total community), with the maximum average density at 1.101 birds/km² in certain coastal locales. There is a clear gradient in these species' density from the coast to the shelf-break, with greater densities closer to shore. Marbled murrelets are more concentrated than the other species of murrelets, particularly very near shore and in the northern portion of the study area. Medium-density areas (0.10-0.50 birds/km²) extend further offshore but remain relatively close to the coastline. High-density areas (more than 1.00 birds/km²) are primarily located within a few kilometers of the coast, with the greatest densities predicted in very coastal locations (again, driven by marbled murrelets in the north).

Density Above 10 Meters: The right panel focuses on seabird-density predictions at elevations above 10 m. Compared to the total density, the densities expected above 10 m are drastically reduced, reflecting the smaller proportion of murrelets flying at these heights. The reduction in density at higher altitudes is consistently about 99.6 percent across the study area, indicating that murrelets are extremely rare (0.4 percent of the 2D density) at these altitudes. The overall mean density expected above 10 m is 0.00006 birds/km², with a maximum average density of 0.0009 birds/km² predicted in offshore areas.

Figure 25: Density Predictions for Federally and/or State Listed as Threatened or Endangered Murrelets Included in the Optimization Framework

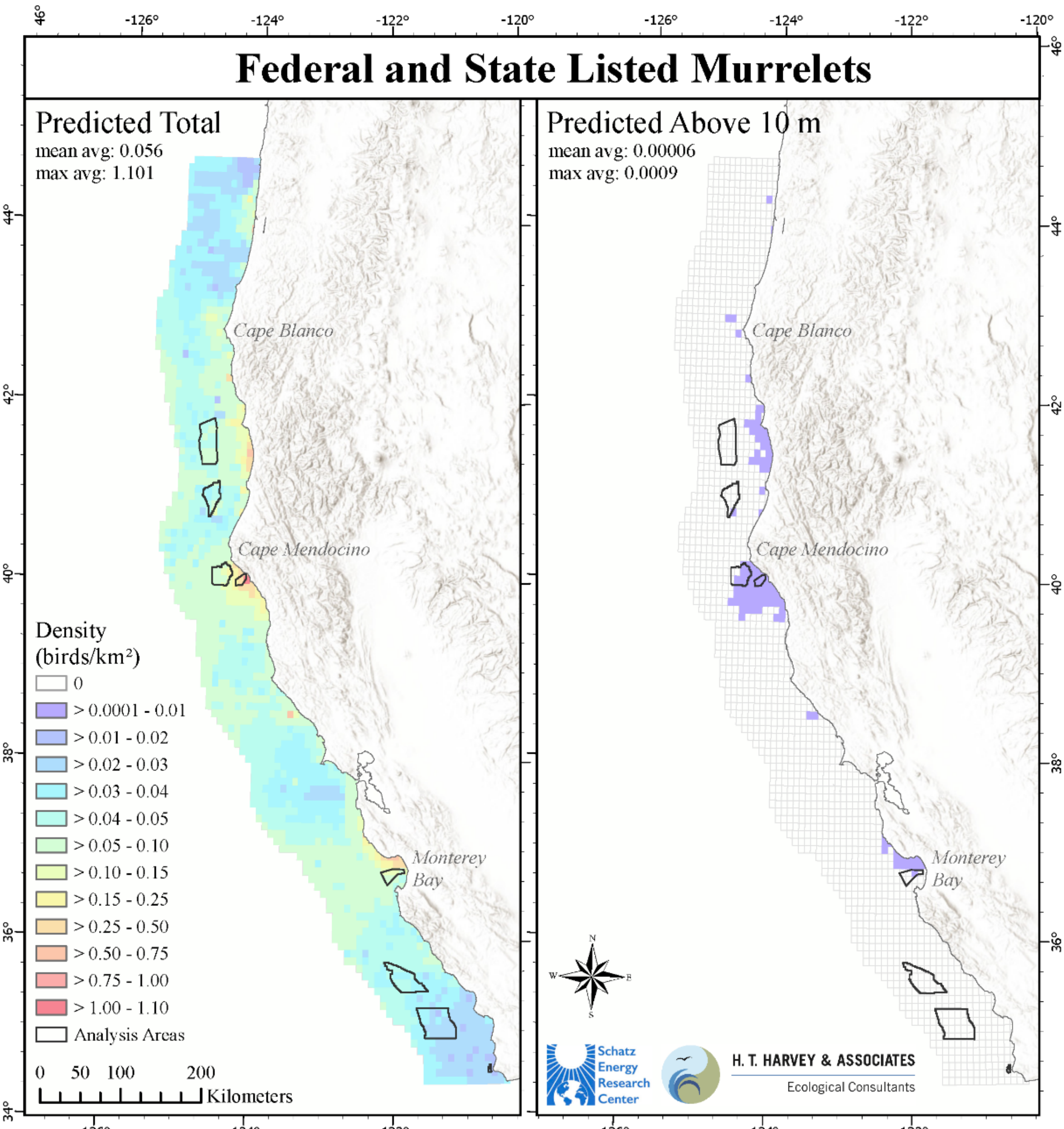

Estimated density of murrelets listed under state and/or federal ESAs at all elevations above the sea surface (left), and at elevations exceeding 10 m (right). Of the 44 seabird taxa included in the Optimization Framework, only two fell under this categorization: marbled murrelet; and Scripps's, Guadalupe, (formerly considered conspecific as Xantus's murrelet, the latter of which was the case during most of the survey period). Marbled murrelets are found primarily very close to shore and the 'Xantus's' murrelets are typically farther offshore, although Scripp's murrelet can occur nearshore in small numbers. This map depicts how seabird density predictions change when

considering all murrelets (left) versus only those flying above 10 m (right). The figure also highlights how seabird densities at rotor swept height vary across space. Black outlines denote References Areas (see Figure 2) highlighted by this study which include planned wind facility locations, notional wind facility locations, and submarine canyon areas known to host a diversity and density of seabirds. All values presented here have units of birds per km².

Source: H. T. Harvey & Associates, Schatz Energy Research Center

Single Turbine Analysis Outcomes

Figure 26 provides a comprehensive visualization of how different locations balance the tradeoffs between federal- and state-listed murrelet species' collision vulnerability and wind energy generation. For these species, alternative sites on the Pareto front can achieve the full range of power generation with bird densities being less than 0.0001 birds/km², while maximum density estimates for this aggregate above 10 m ASL reach around 0.0001 birds/km² (or 1 bird every 10,000 km²). This Pareto curve has a sharp knee that would indicate that seabird and power generation objectives are largely not in conflict.

Of all the aggregates, the outcome for federal- and state-listed murrelets is most different from that of the All Species aggregate. Key differences include:

1. Unlike the analysis focused on all species in the framework, the analysis focused on murrelets depicts areas near the Pareto front for listed murrelets as being more diffusely spread across the study area, with areas meeting balanced objectives shifting to southerly regions;
2. Areas off Cape Mendocino are most optimal for power generation;
3. Areas offshore are generally better for achieving the lowest densities of this particular aggregate, which makes sense given that this particular aggregate is dominated by marbled murrelets, which occur very close to shore compared to the other, far less abundant, murrelet species that occur in waters off the shelf; and
4. Areas near Point Conception, just north of San Francisco Bay, and localized spots near the California-Oregon border are categorized as having a good balance of power generation potential and listed bird vulnerability.

Figure 26: Pareto Optimality Outcomes for Federal and State ESA-listed Murrelets

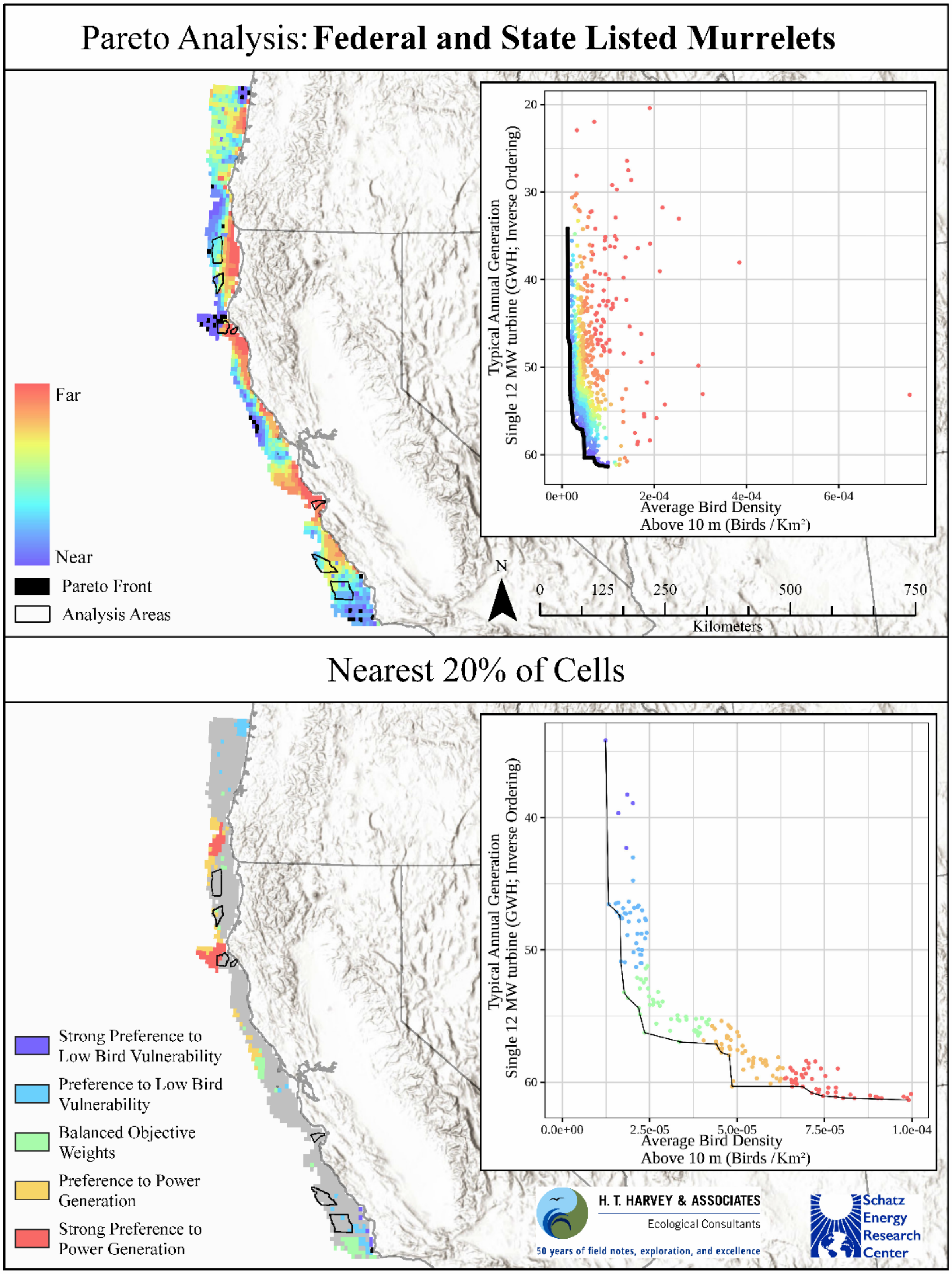

Pareto optimality analysis for federal- and state-listed murrelets, highlighting the tradeoffs between density above 10 m and power generation for a single 12-MW turbine. The top panel shows the spatial distribution of the Pareto front, with colors indicating the distance of each cell

from this frontier. The inset graph within the top panel presents the Pareto front in solution space, with each point representing a potential turbine location and colored by its distance from the Pareto front. The bottom panel highlights the top 20 percent of cells closest to the Pareto front, categorizing sites based on their tendency to prioritize either low bird vulnerability, power generation, or a balanced outcome.

Source: Schatz Energy Research Center, H. T. Harvey & Associates

Wind Facility Analysis Outcomes

When evaluating total facility metrics (Figure 27, left panel), as with the other aggregates, a key pattern that emerged was locations capable of supporting a larger number of turbines exhibited greater total power generation and increased bird vulnerabilities. Notably, the Humboldt WEA, Morro Bay WEA, and former Diablo Canyon area are on the Pareto front, with the notional Crescent City and Cape Mendocino areas positioned to the right due to their relatively larger bird densities. Given the steepness of this Pareto front, from the perspective of the federal- and state-listed murrelet species included in the Optimization Framework, Diablo Canyon appears especially balanced. It nearly matches Humboldt's low total vulnerability of listed species while generating the highest amount of power among the scenarios.

When considering per-turbine metrics (Figure 27, right panel), all scenarios except the Monterey System and Delgada Canyon fall on the Pareto front. These seabird areas show low per turbine generation and relatively high densities of federal- and state-listed murrelets. Similar to the analysis considering additive total facility metrics (left panel), the Pareto front for per-turbine metrics (right panel) is very steep, indicating that most scenarios perform similarly in terms of seabird vulnerability, with the main differences being in power generation. Cape Mendocino represents a slight exception with a modest increase in bird density compared to the nearest alternative.

When evaluating total facility metrics (Figure 27, left panel), a key pattern that emerged was locations capable of supporting a larger number of turbines exhibited both greater total power generation and increased bird vulnerabilities. This illustrates the inherent tradeoff between scaling up wind energy capacity and the associated risks to these seabirds. As facilities increase in size, the cumulative impact on seabird populations is likely to increase, though not necessarily in a linear fashion.

This highlights the importance of evaluating total and per-turbine metrics to understand the potential impacts of wind energy facilities on seabird populations.

Figure 27: Pareto Analysis for Reference Areas Based on Federal and State ESA-listed Murrelet Species

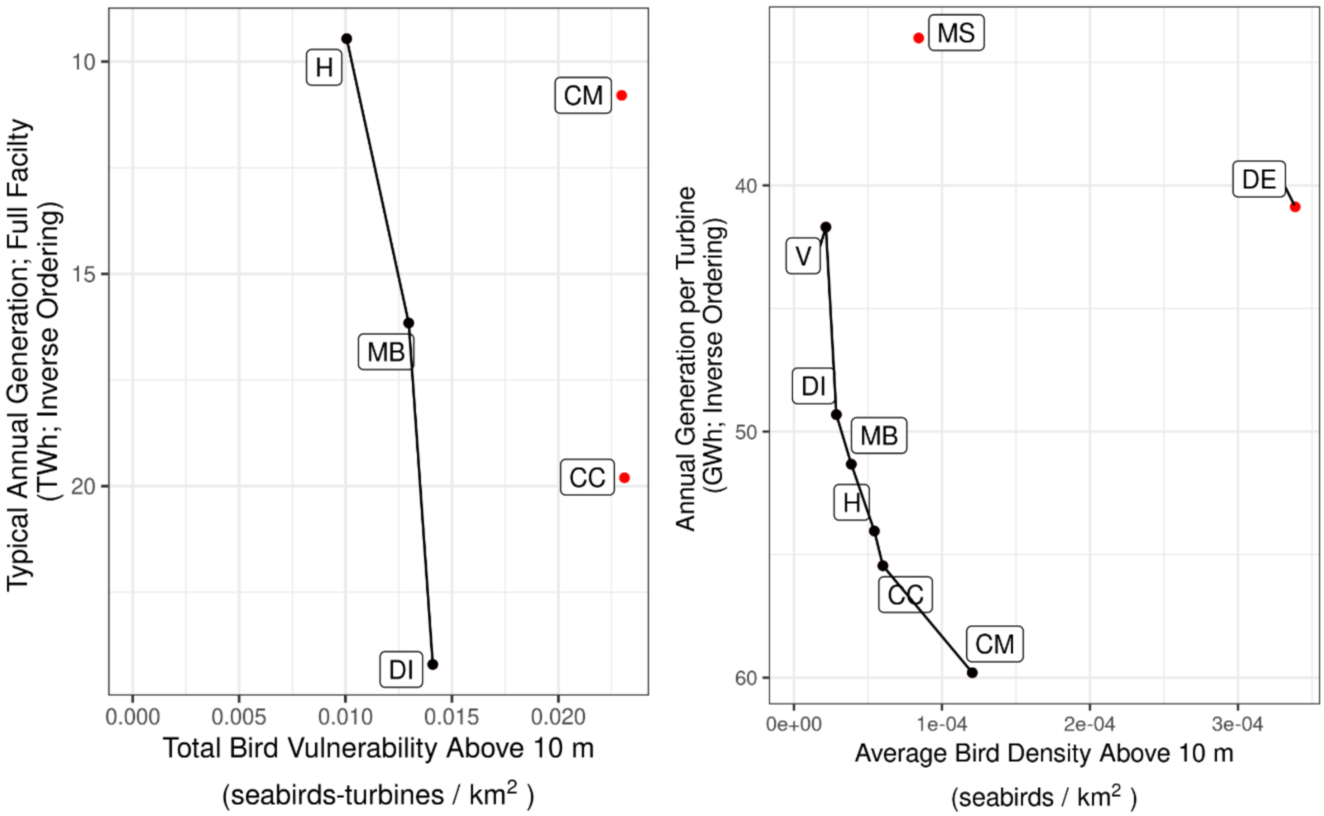

Pareto optimality analysis curves for Federal and State ESA-listed murrelets, illustrating the tradeoffs between density above 10 m and power generation for different wind facility scenarios simulated at the reference areas. The left panel compares total bird vulnerability (sum of birds per turbine per km²) with typical annual generation (TWh/yr) for the full facility, while the right panel compares average bird density (birds/km²) above 10 m with annual generation per turbine (GWh/yr). Black points on the Pareto front indicate scenarios that offer the best tradeoffs between minimizing bird density and maximizing power generation. A total of eight sites were included: Crescent City (CC), Cape Mendocino (CM), Delgada Canyon (DE), Diablo Canyon (DI), Humboldt (H), Morro Bay (MB), Monterey System (MS), and Vandenberg (V).

Source: Schatz Energy Research Center

Validation of Methods

Wind Speed: Wind speed models were validated by comparing them with real-world measurements from floating wind-profiling LiDAR buoys in the BOEM-designated Humboldt and Morro Bay WEAs. Despite technical issues with the Humboldt buoy, leading to some data gaps, modeled wind speeds were found to be approximately 1 m/s higher than actual measurements at turbine hub heights, after adjusting for unusually high wind speeds during the validation period. This overestimation of wind speed led to overestimating power generation and underestimating rates of seabirds flying above 10 m. However, the magnitude of these effects was small and consistently applied to the study area, so the relative differences in predictions from the areas addressed by this study are minor.

Seabird Density: The seabird density predictions were validated using cross-validation, a process that systematically removed one data point at a time, predicted its value, and compared it to actual observations, adjusting the model to minimize prediction errors. This process ensured that seabird density predictions were accurate, providing reliable data to assess the potential impacts of OSW developments on seabird populations.

Power Generation: The Power Generation Model's predictions were compared with real wind speed data from the LiDAR buoys. Despite the anomaly of high wind speeds at Humboldt, researchers found that the model overestimated average power generation by 600 kilowatts at Humboldt and 470 kilowatts at Morro Bay, representing 5 percent and 3.9 percent of turbine capacity, respectively. This validation highlights the need to correct potential biases in the power generation forecasts to ensure reliable energy output predictions for OSW projects.

CHAPTER 4: Conclusion

Broad Patterns

Extensive datasets of seabird observations and the offshore windscape were integrated to address a critical gap in understanding the tradeoff between OSW energy development and seabird conservation by incorporating the vertical component of seabird flight. Unlike previous 2D density and risk analyses (such as Leirness et al. 2021 and Adams et al. 2016), this research integrated a 3D framework, adding flight height to 2D seabird density and providing visualizations to answer: How have seabirds historically used airspace that could potentially become occupied by the RSZs of OSW energy developments?

Seabird Community: California’s seabird community is diverse, encompassing 18 distinct FGs and 44 regularly observed taxa, with 109 total taxa observed in scientific at-sea surveys from 1980 to 2016. The majority (about 92 percent) of this community is predicted to fly near the sea surface (below 10 m). Most FGs are expected to fly below the RSZ while at sea and, thus, are extremely unlikely to fly at collision risk heights, including birds in FGs such as storm-petrels, phalaropes, cormorants, and small and medium alcids.

Horizontal Patterns: The community of birds nearshore is expected to have a different composition and density compared to those further offshore due to different foraging strategies and habitat preferences. Nearly all locally breeding birds are found over the shelf and closer to the coast, while most birds beyond the shelf-break are migratory species that exhibit seasonality in their presence off California (Ainley 1976, Briggs et al. 1987).

Vertical Patterns: Among FGs that are expected to fly at RSZ-height, the likelihood is expected to vary as a function of wind speed, ranging from 0 to 100 percent for larger diving shearwaters and from 0 to 35–40 percent for large gulls. FGs with the greatest propensity for individuals to fly at collision risk heights include gulls and large diving shearwaters. Gulls are frequently observed above 10 m and, importantly, gulls and close taxonomic relatives such as terns have well-documented interactions with wind turbines from OSW sites in the Atlantic — some showing attraction and others avoidance (van Bemmelen et al. 2023, Degraer et al. 2023, Vanermen et al. 2013) — but are generally very adept at avoiding collision (Cook et al. 2018). Sooty shearwaters represent a significant proportion of dynamic soaring species that are abundant in the CCS and require further research to understand their interactions with OSW infrastructure.

Overlap with Areas of Best Wind Resource: Winds are most favorable offshore and to the north of the study area, and RSZs aren’t expected to extend below 25 m ASL. Seabirds are most concentrated nearshore, to the south, and below 10 m. Recently published data on seabird passage rates at the Humboldt WEA suggest that 21.2 percent of the seabird community was moving at collision risk height (above 30 m ASL) during an 82-day observation period (May to August 2021) (Schneider et al. 2024a), compared to 6.9 percent (above 10 m ASL) in this study. However, it is important to distinguish the difference in the derivation of these results: the former represents raw data, and the latter represents the percent average density based on wind speeds over a 20-year period. In any study based on human observation of seabirds, an inherent bias is likely because human observers are likely unable to see seabirds at night or perhaps even in the upper extent of the RSZ, which leads to undercounting and an underestimation of densities for the highest of flying birds.

Implications for OSW Developments

This study provides the first explicit predictions of the seabird community likely to be present at heights above 10 m ASL, including those overlapping RSZs. The framework's predictions allow for the quantification of the vulnerable species within the seabird community, aiding in identifying broad patterns of risk and the magnitude of potential vulnerability across areas being considered for OSW development. Even if predictions of the magnitude of birds present in the study area are biased, the relative differences between sites should be stable and comparisons are valid. This research offers insights about the relative risk of various locations across the California coastal ocean. The ongoing collection and integration of new data, including advancements in tracking technologies, can continuously update and refine the outputs of the Optimization Framework, ensuring responsiveness to emerging ecological data (such as Schneider et al. 2024a). The predictions provided by the Optimization Framework offer insight into the flight heights of various seabirds off California, as well as an indication of the possible magnitude of passage at collision risk heights. Included are predictions for areas that may not have been otherwise surveyed. This information can inform project siting, improve understanding of impacts needed for projects to receive permits, define the need for pre- and post-construction surveys, and identify potential needs for mitigation. Without this information, there would be greater uncertainty of the potential magnitude of impacts, potentially resulting in costly and longer-term pre-construction survey requirements and longer time frames to achieve permitting.

Framework Limitations

Rare species: The framework was able to include only a subset of rare species. Here, species classified as federal- and state-listed species are highlighted but a few species — and only murrelet species — were sufficiently observed to be included in the framework. Rare species can be aggregated in various ways (such as International Union for Conservation of Nature Red List versus ESA-listed) but, regardless of how these rare species are treated, they are often too rare to be detected at historical levels of at-sea survey effort and are thus not appropriate to include in this analysis due to lack of data. Importantly, many seabird species with this status, including the short-tailed albatross and the Hawaiian petrel, are dynamic soarers and thus much more likely to fly at RSZ height at faster wind speeds. However, their rarity during the period the surveys were conducted means they would require additional data in the study area, potentially targeting areas where these species are likely to occur. Despite the importance of rare birds in the permitting process, framework predictions based on the ”all species” aggregate are insensitive to their inclusion due to the small numbers of these species during the study period.

Ongoing changes in species distribution and abundance: Observations during the survey time period (1980–2016) indicate changes in the abundance of some seabirds, such as a decrease in sooty shearwaters (Veit et al. 1997), and an increase in common murres (Ainley et al. 2021, Warzybok et al. 2018) and brown pelicans (Sheilds 2020). Additionally, historically rare birds have increased in waters off California (such as sulids like brown boobies; Russell 2024).

Gaps in observations: Challenges in obtaining sufficient site- and species-specific data solely with human observers highlight several gaps. These include the absence of nocturnal flight observations despite seabird activity at night (see Schneider et al. 2024a) and the potential to miss short-lived migration pulses (as noted for certain species of gulls). High-resolution understanding of passage rates and their variation requires more than broad-scale at-sea surveys following historical monitoring protocols. Future efforts, including the development and use of autonomous bird-tracking technologies (such as the ThermalTracker-3D) along the U.S. West Coast (Schneider et al. 2024a), can help fill these gaps.

Estimating flight height: Human observers likely cannot detect birds throughout the entire RSZ, which extends up to 260 m (850 ft) ASL, and they have difficulty making accurate estimation of height as altitudes and distance from the observer increase (thus, this study uses coarse groupings of altitude). However, the flight heights binned in the present study were assessed by observers on the bridges of ocean-going ships to allow eye height to be above 10 m. Therefore, this study's flight height data rely on conservative thresholds for the RSZ-height. The 10-m ASL threshold may appear conservative, and preliminary results of new technologies deployed at a site in the Humboldt WEA off California (Matzner et al. 2022, Schneider et al. 2024a) confirm that about half of the birds stay within the first 10 m of airspace, at least during the period of data collection. However, results also suggest that birds flying between 10 and 260 m ASL may have been undercounted or missed by human observers.

Collision vulnerability model versus CRM: Developing a comprehensive CRM requires additional parameters, many of which can be determined only once project planning is well underway (such as the number and placement of turbines). Furthermore, much remains to be learned about facility-level parameters such as size and shape and their impact on bird behavior and, ultimately, collision risk; larger facilities may result in attraction, deterrence, or no change. The 3D framework offers a broad quantification of the spatial variability in the composition and magnitude of seabirds likely to fly at heights that increase their potential to encounter RSZs, thereby increasing their vulnerability to turbine blade collisions. Although it’s not a complete CRM, this framework provides essential input data, including density estimates and flight height information across the CCS, even predicting densities in regions that have not been directly surveyed. This integration aids in better understanding and mitigating potential risks, ensuring more accurate assessments and informed decision-making for OSW developments.

Long-term versus short-term expectations: The study provides a good sense of the overall, long-term magnitude of possible exposure and spatial variation in risk. However, it does not capture the extremity of conditions present for brief periods. Information about the upper limits of densities expected at RSZ-height was likely lost by using averages.

Next Steps

The outcome of this project can be used for immediate decision-making and environmental analyses. Both are ongoing off the U.S. West Coast. For example, BOEM released a draft of the California Offshore Wind Draft Programmatic Environmental Impact Statement in November 2024 for a 90-day public comment period (BOEM 2024). All seabird predictions are available online for downstream analyses (Wallach et al. 2024), including expanded site-selection analyses that consider objectives in addition to power generation and seabird collision vulnerability and further refinement to ongoing analyses to better predict impacts ahead of construction.

Future efforts should focus on integrating recent observational data, especially targeting rare and historically difficult-to-observe species, like the short-tailed albatross and the Hawaiian petrel. Autonomous tracking technologies, such as ThermalTracker3D employed for extended periods, could fill gaps in nocturnal flight observations and migration pulses, enhancing the accuracy of seabird flight height and passage rate estimates across the full extent of RSZs. Developing comprehensive CRMs will require detailed and site-specific data collection, ideally capturing a representative spectrum of risk periods. Expanding the framework to other regions in the Pacific, including more northerly sections of the U.S. West Coast, could provide insights into seabird collision vulnerability and OSW power generation potential across the broader CCS. Continually refining the Multi-objective Optimization Framework with new data and technologies will result in a framework that can help inform siting decisions for OSW development in the CCS in a way that directly considers seabirds.

GLOSSARY AND LIST OF ACRONYMS

Term	Definition
2D	2 dimensions of space, including horizontal (x, y) components
3D	3 dimensions of space, including horizontal (x, y) and vertical (z) components
ASL	Above sea level
BOEM	Bureau of Ocean Energy Management
Call Area	An area established by BOEM for initial assessment prior to designation as a WEA
CC, CM, DE, DI, H, MB, MS, V (reference areas)	Crescent City, Cape Mendocino, Delgada Canyon, Diablo Canyon, Humboldt, Morro Bay, Monterey System, Vandenberg
CCS	California Current System
CEC	California Energy Commission
CRM	Collision risk model
Density	Number of individuals per area
EPIC	Electric Program Investment Charge
ESA	Endangered Species Act
FG	Flight group
Full buildout	An estimate of maximum feasible installed capacity of a reference area
km, m, m/s	Kilometers, meters, meters per second
LIDAR	Light Detection and Ranging
MW, GW, GWh, GWh/yr, TWh/yr	Megawatt, gigawatt, gigawatt-hour, gigawatt-hour per year, terawatt-hour per year
nm	nautical miles
NREL	National Renewable Energy Laboratory
OCS	Outer continental shelf
OSW	Offshore wind
Pareto optimization	A graphical form of multi-variate optimization
Reference Areas	Sites used to simulate various wind facility scenarios
RSZ	Rotor-swept zone
WEA	Wind Energy Area
Windscape	The comprehensive distribution of wind speeds at a site

References

Adams, J., E. C. Kelsey, J. J. Felis, and D. M. Pereksta. 2016. *Collision and displacement vulnerability among marine birds of the California Current System associated with offshore wind energy infrastructure* (Open-File Report 2016-1154). Prepared in cooperation with Bureau of Ocean Energy Management (OCS Study, BOEM 2016-043). https://doi.org/10.3133/ofr20161154.

Ainley, D. G. 1976. "The occurrence of seabirds in the coastal region of California." *Western Birds* 7: 33–68.

Ainley, D. G., D. N. Nettleship, and A. E. Storey. 2021. "Common murre (*Uria aalge*)," version 2.0. In *Birds of the World*, edited by S. M. Billerman, P. G. Rodewald, and B. K. Keeney. Cornell Lab of Ornithology. https://doi.org/10.2173/bow.commur.02.

Ainley, D. G., E. L. Porzig, D. Zajanc, and L. B. Spear. 2015. "Seabird flight behavior and height in response to altered wind strength and direction." *Marine Ornithology* 43: 25–36.

AWS Truepower. 2014. Loss and uncertainty methods.

Beiter, P., W. Musial, P. Duffy, A. Cooperman, M. Shields, D. Heimiller, and M. Optis. 2020. *The cost of floating offshore wind energy in California between 2019 and 2032*. National Renewable Energy Laboratory. https://www.nrel.gov/docs/fy21osti/77384.pdf.

BOEM (Bureau of Ocean Energy Management). 2024. *California offshore wind draft programmatic environmental impact statement.* November 2024. Volume I: Chapters 1–4. BOEM Publication 2024-063. https://www.boem.gov/sites/default/files/documents/renewable-energy/state-activities/2024_1021_CA_PEIS_Vol_I_508c_0.pdf.

Briggs, K.T., William Tyler, D.B. Lewis, and D.R. Carlson. 1987. "Bird communities at sea off California: 1975 to 1983." *Studies in Avian Biology*, 11: 1-74. https://www.researchgate.net/publication/284513093_Bird_communities_at_sea_off_California_1975_to_1983

California State Lands Commission. 2021. Offshore wind applications. January 25. https://www.slc.ca.gov/renewable-energy/offshore-wind-applications/.

Clarke, E. D., L. B. Spear, M. L. McCracken, F. F. C. Marques, D. L. Borchers, S. T. Buckland, and D. G. Ainley. 2003. "Validating the use of generalized additive models and at-sea surveys to estimate size and temporal trends of seabird populations." *Journal of Applied Ecology*, 40 (2): 278–292.

Cook, A. S. C. P., E. M. Humphreys, F. Bennet, E. A. Masden, N. H. K. Burton. 2018. "Quantifying avian avoidance of offshore wind turbines: Current evidence and key knowledge gaps." *Marine Environmental Research* 140: 278–288. https://doi.org/10.1016/j.marenvres.2018.06.017.

Croll, D. A., B. Marinovic, S. Benson, F. P. Chavez, N. Black, R. Ternullo, and B. R. Tershy. 2005. "From wind to whales: Trophic links in a coastal upwelling system." *Marine Ecology Progress Series* 289: 117–130.

Degraer, S., R. Brabant, B. Rumes, and L. Vigin, eds. 2023. *Environmental impacts of offshore wind farms in the Belgian part of the North Sea: Progressive insights in changing species distribution patterns informing marine management. Memoirs on the Marine Environment*. Royal Belgian Institute of Natural Sciences. https://biblio.naturalsciences.be/library-1/rbins-staff-publications-2023/bookreference.2024-02-01.0870539794.

Flint, S., R. deMesa, P. Doughman, and E. Huber. 2022*. Offshore wind development off the California coast: Maximum feasible capacity and megawatt planning goals for 2030 and 2045*. California Energy Commission. CEC-800-2022-001-REV.

Ford, G. R., S. Terrill, J. Casey, D. Shearwater, S. R. Schneider, L. T. Ballance, L. Terrill, et al. 2021. "Distribution patterns and population size of the ashy storm petrel *Oceanodroma homochroa*." *Marine Ornithology* 49: 193–204.

Freeman, J., J. Jorgenson, P. Gilman, and T. Ferguson. 2014*. Reference manual for the System Advisor Model's wind power performance model.* NREL/TP-6A20-60570. National Renewable Energy Laboratory. https://docs.nrel.gov/docs/fy14osti/60570.pdf.

Gaertner, Evan, Jennifer Rinker, Latha Sethuraman, Frederik Zahle, Benjamin Anderson, Garrett Barter, Nikhar Abbas, Fanzhong Meng, Pietro Bortolotti, Witold Skrzypinski, George Scott, Roland Feil, Henrik Bredmose, Katherine Dykes, Matt Shields, Christopher Allen, and Anthony Viselli. 2020. Definition of the IEA Wind 15-Megawatt Offshore Reference Wind Turbine. Golden, CO: National Renewable Energy Laboratory. NREL/TP-5000-75698. https://www.nrel.gov/docs/fy20osti/75698.pdf.

Leirness, J. B., J. Adams, L. T. Ballance, M. Coyne, J. J. Felis, T. Joyce, D. M. Pereksta, et al. 2021. *Modeling at-sea density of marine birds to support renewable energy planning on the Pacific Outer Continental Shelf of the contiguous United States.* OCS Study BOEM 2021-014. U.S. Department of the Interior, Bureau of Ocean Energy Management. https://repository.library.noaa.gov/view/noaa/49073#moretextPAmods.subject_name.

Masden, E. A., and A. S. C. P. Cook. 2016. "Avian collision risk models for wind energy impact assessments." *Environmental Impact Assessment Review* 56: 43–49.

Matzner, S., T. E. Warfel, R. Hull, and N. Williams. 2022. *ThermalTracker-3D offshore validation technical report*. Contract DE-AC05-76RL01830. Prepared for the U.S. Department of Energy by Pacific Northwest National Laboratory. https://tethys.pnnl.gov/publications/thermaltracker-3d-offshore-validation-technical-report.

NREL (National Renewable Energy Laboratory). 2023. "Wind toolkit data downloads: Offshore CA data download." https://developer.nrel.gov/docs/wind/wind-toolkit/offshore-ca-download/.

Nur, N., J. Jahncke, M. P. Herzog, J. Howar, K. D. Hyrenbach, J. E. Zamon, D. G. Ainley, et al. 2011. "Where the wild things are: Predicting hotspots of seabird aggregations in the California Current System." *Ecological Applications* 21 (6): 2241-2257. https://doi.org/10.1890/10-1460.1.

Pacific Ocean Energy Trust. 2021. "Webinar – Subsea transmission solutions for OSW between California and Oregon." https://pacificoceanenergy.org/2021/04/19/webinar-subsea-transmission-solutions-for-osw-between-california-and-oregon/.

Pennycuick, C. J. 1987a. "Flight of seabirds." In *Seabirds: Feeding ecology and role in marine ecosystems,* edited by J. P. Croxall: 43–62. Cambridge University Press. https://research-information.bris.ac.uk/en/publications/flight-of-seabirds.

Pennycuick, C. J. 1987b. "Flight of auks (Alcidae) and other northern seabirds compared with southern procellarhformes: Ornithodolite observations." *Journal of Experimental Biology* 128 (1): 335–347. https://journals.biologists.com/jeb/article-abstract/128/1/335/5067/Flight-of-Auks-Alcidae-and-Other-Northern-Seabirds?redirectedFrom=fulltext.

Rose, A., D. Wei, and A. Einbinder. 2022. "The co-benefits of California offshore wind electricity." *The Electricity Journal* 35 (7): 107167.

Russell, T. 2024. Seabird habitat use within the California Current (PhD dissertation, University of California, San Diego).

Russell, T. M., A. R. Szesciorka, T. Joyce, D. G. Ainley, and L. T. Ballance. 2023. "National marine sanctuaries capture enhanced abundance and diversity of the California Current Ecosystem avifauna." *Journal of Marine Systems* 240 (1) (1038887): 1–16.

Schneider, S. R., S. H. Kramer, S. B. Bernstein, S. B. Terrill, D. G. Ainley, and S. Matzner. 2024a. "Autonomous thermal tracking reveals spatiotemporal patterns of seabird activity relevant to interactions with future floating offshore wind facilities." *Frontiers in Marine Science*. https://doi.org/10.3389/fmars.2024.1346758.

Schneider, S. R., E. Wallach, C. Chamberlin, S. B. Bernstein, S. Trush, D. G. Ainley, S. B. Terrill, et al. 2024b. *Seabirds in 3D: A framework to evaluate collision vulnerability with future offshore wind developments* (California Energy Commission Interim Project Task Report). Schatz Energy Research Center, Humboldt, CA.

Severy, M., C. Ortega, C. Chamberlin, and A. Jacobson. 2020. *Wind speed resource and power generation profile report*. September. California North Coast Offshore Wind Studies. Prepared for the U.S. Department of the Interior, Bureau of Ocean Energy Management by Schatz Energy Research Center, Humboldt, California.

Shields, M. 2020. "Brown pelican (*Pelecanus occidentalis*)," version 1.0. In *Birds of the World,* edited by A. F. Poole. Cornell Lab of Ornithology. https://doi.org/10.2173/bow.brnpel.01.

Skov H., S. Heinänen, T. Norman, R. M. Ward, S. Mendez-Roldan, and I. Ellis. 2018*. ORJIP Bird Collision Avoidance Study*. Final Report - April 2018. NIRAS and DHI on behalf of The Carbon Trust (U.K). https://tethys.pnnl.gov/sites/default/files/publications/Skov-et-al-2018.pdf.

Spear, L. B., N. Nur, and D. G. Ainley. 1992. "Estimating absolute densities of flying seabirds using analyses of relative movement." *The Auk* 109 (2): 385–389.

Spear, L. B., D. G. Ainley, S. N. G. Howell, B. D. Hardesty, and S. W. Webb. 2004. "Reducing biases affecting at-sea surveys of seabirds: Use of multiple observer teams." *Marine Ornithology* 32 (2): 147–157.

Tjørnløv R. S., H. Skov, M. Armitage, M. Barker, J. B. Jørgensen, L. O. Mortensen, K. Thomas, T. Uhrenholdt. 2023. *Resolving Key Uncertainties of Seabird Flight and Avoidance Behaviours at Offshore Wind Farms: Final report for the study period 2020-2021*. Report by DHI A/S for Vattenfall, Horsholm, Denmark. Project No. 11820296.

U.S. Energy Information Administration. 2022. "Wind was second-largest source of U.S. electricity generation on March 29." April 14. https://www.eia.gov/todayinenergy/detail.php?id=52038#:~:text=In%20September%202019%2C%20U.S.%20wind.

van Bemmelen, R. S. A., J. J. Leemans, M. P. Collier, R. M. W. Green, R. P. Middelveld, C. B. Thaxter, and R. C. Fijn. 2023. "Avoidance of offshore wind farms by sandwich terns increases with turbine density." *Ornithological Applications* 126. doi:10.1093/ornithapp/duad055.

Vanermen, N., E. W. M. Stienen, W. Courtens, T. Onkelinx, M. Van de Walle, and H. Verstraete. 2013. *Bird monitoring at offshore wind farms in the Belgian part of the North Sea - Assessing seabird displacement effects*. Rapporten van het Instituut voor Natuur- en Bosonderzoek (INBO.R.2013.755887). Instituut voor Natuur- en Bosonderzoek. https://www.researchgate.net/publication/259791361_Bird_monitoring_at_offshore_wind_farms_in_the_Belgian_part_of_the_North_Sea_-_Assessing_seabird_displacement_effects.

Veit, R. R., J. A. McGowan, D. G. Ainley, T. R. Wahl, and P. Pyle. 1997. "Apex marine predator declines ninety percent in association with changing oceanic climate." *Global Change Biology* 3 (1): 23–28. https://www.researchgate.net/publication/230225577_Apex_marine_predator_declines_ninety_percent_in_association_with_changing_oceanic_climate.

Wallach, E., S. R. Schneider, D. G. Ainley, S. Terrill, G. Ford, J. Santora, S. Kramer, J. Casey, C. Chamberlin, and A. Jacobson. 2024. "3D seabird density estimates" [Data set]. *Zenodo*. https://doi.org/10.5281/zenodo.11620539.

Williams, K., J. Gulka, A. Cook, R. Diehl, A. Farnsworth, H. Goyert, C. Hein, P. Loring, D. Mizrahi, I. Petersen, T. Peterson, K. Press, and I. Stenhouse. 2024. "A framework for studying the effects of offshore wind energy development on birds and bats in the Eastern United States." *Frontiers in Marine Science* 11. https://doi.org/10.3389/fmars.2024.1274052.

Warzybok, P., J. A. Santora, D. G. Ainley, R. W. Bradley, J. C. Field, P. J. Capitolo, R. D. Carle, et al. 2018. "Prey switching and consumption by seabirds in the central California Current upwelling ecosystem: Implications for forage fish management." *Journal of Marine Systems* 185: 25–39.

Project Deliverables

Four interim project reports are available upon request by submitting an email to pubs@energy.ca.gov or by following the links provided below.

- Task 2: Offshore Wind Speed Report
- Task 3: 3D Seabird Risk Assessment Report, Seabirds in 3D: A Framework to Evaluate Collision Vulnerability with Future Offshore Wind Developments--Estimating Collision Vulnerability of the Seabird Community Across a Segment of the California Current System, and Associated 3D Spatial Seabird Occurrence Spatial Data Layers
    - Report: https://schatzcenter.org/pubs/2024-OSW-R1-Seabirds-HTHarveyandSchatzCenter.pdf
    - Spatial Layers: https://doi.org/10.5281/zenodo.11620539
- Task 4: Offshore Wind Power Generation Scenarios Report
- Task 5: Seabirds in 3D: A Framework to Evaluate Collision Vulnerability with Future Offshore Wind Developments Assessing Tradeoffs between Seabird Density at Collision Risk Height and Wind Facility Performance

CALIFORNIA ENERGY COMMISSION

CALIFORNIA NATURAL RESOURCES AGENCY

ENERGY RESEARCH AND DEVELOPMENT DIVISION

APPENDIX A: Seabird Community Predictions

July 2025 | CEC-500-2025-037

APPENDIX A: Seabird Community Predictions

Table A-1: All Seabirds Included in the Predictions of the Multi-objective Optimization Project

ID	Flight Group	Common Name	Latin Name	Counted Seabirds (%)	Predicted Seabirds (%)	Predicted Seabirds above 10 m (%)	Effort with Detections (km^2)
1	Small Albatrosses	Black-footed Albatross	*Phoebastria nigripes*	0.60	0.80	5.7	2,489
2	Small Albatrosses	Laysan Albatross	*Phoebastria immutabilis*	0.00	0.00	5.7	183
3	Fulmars	Northern Fulmar	*Fulmarus glacialis*	1.10	1.70	1.3	3,674
4	Surface-Feeding Shearwaters	Buller's Shearwater	*Ardenna bulleri*	0.50	0.50	3.6	951
5	Surface-Feeding Shearwaters	Pink-footed Shearwater	*Ardenna creatopus*	0.80	1.00	3.7	2,074
6	Larger Diving Shearwaters	Sooty Shearwater	*Ardenna grisea*	33.80	27.30	5.7	8,001
7	Larger Diving Shearwaters	Short-tailed Shearwater	*Ardenna tenuirostris*	0.00	0.00	5.5	108
8	Smaller Diving Shearwaters	Black-vented Shearwater	*Puffinus opisthomelas*	0.20	0.30	0.4	199
9	Storm-Petrels	Fork-tailed Storm-Petrel *	*Hydrobates furcata*	1.00	1.60	0	789
10	Storm-Petrels	Leach's Storm-Petrel	*Hydrobates leucorhous*	0.80	0.60	0	2,289
11	Storm-Petrels	Ashy Storm-Petrel *	*Hydrobates homochroa*	0.20	0.20	0	695
12	Pelicans	Brown Pelican	*Pelecanus occidentalis*	0.50	0.50	23.9	1,580
13	Phalaropes	Phalaropes	*Phalaropus spp.*	7.70	7.80	1.3	4,185
14	Skuas	Long-tailed Jaeger	*Stercorarius longicaudus*	0.10	0.00	21.3	368
15	Skuas	Parasitic Jaeger	*Stercorarius parasiticus*	0.00	0.00	21.3	363
16	Skuas	Pomarine Jaeger	*Stercorarius pomarinus*	0.10	0.10	21.3	727
17	Skuas	South Polar Skua	*Stercorarius McCormick*	0.00	0.00	21.3	145
18	Large Gulls	California Gull	*Larus californicus*	5.50	5.80	35.4	4,601
19	Large Gulls	Herring Gull	*Larus argentatus*	0.80	1.40	35.5	1,789
20	Large Gulls	Western Gull	*Larus occidentalis*	3.70	3.60	35.5	8,400

ID	Flight Group	Common Name	Latin Name	Counted Seabirds (%)	Predicted Seabirds (%)	Predicted Seabirds above 10 m (%)	Effort with Detections (km^2)
21	Large Gulls	Glaucous-winged Gull	*Larus glaucescens*	0.30	0.50	35.5	1,200
22	Large Gulls	Heermann's Gull	*Larus heermanni*	0.30	0.40	35.4	1,008
23	Medium Gulls	Black-legged Kittiwake	*Rissa tridactyla*	1.00	1.40	37.4	1,508
24	Medium Gulls	Short-billed Gull	*Larus brachyrhynchus*	0.00	0.00	37.5	111
25	Small Gulls	Bonaparte's Gull	*Chroicocephalus philadelphia*	0.60	0.90	21.9	524
26	Small Gulls	Sabine's Gull	*Xema sabini*	0.30	0.30	21.9	645
27	Terns	Arctic Tern	*Sterna paradisaea*	0.30	0.20	42.3	520
28	Terns	Caspian Tern	*Hydroprogne caspia*	0.00	0.00	42.5	167
29	Terns	Elegant Tern	*Thalasseus elegans*	0.20	0.10	42.8	307
30	Cormorants	Brandt's Cormorant	*Urile penicillatus*	1.80	2.00	2.7	2,399
31	Cormorants	Double-crested Cormorant	*Nannopterum auritum*	0.00	0.00	2.7	150
32	Cormorants	Pelagic Cormorant	*Urile pelagicus*	0.00	0.00	2.7	272
33	Large Alcids	Common Murre	*Uria aalge*	20.90	23.10	0.9	8,725
34	Large Alcids	Tufted Puffin *	*Fratercula cirrhata*	0.00	0.00	1	110
35	Medium Alcids	Rhinoceros Auklet	*Cerorhinca monocerata*	2.00	2.40	0.1	3,833
36	Medium Alcids	Pigeon Guillemot	*Cepphus columba*	0.10	0.10	0.1	281
37	Small Alcids	Cassin's Auklet *	*Ptychoramphus aleuticus*	4.30	5.50	0.1	4,282
38	Small Alcids	Marbled Murrelet **	*Brachyramphus marmoratus*	0.10	0.10	0.1	346
39	Small Alcids	Scripps's, Guadalupe, Craveri's Murrelet **	*Synthliboramphus spp.*	0.00	0.00	0.1	108
40	Loons, Grebes, Ducks	Western and Clarke's Grebes	*Aechmophorus spp.*	6.80	5.70	7.9	2,150
41	Loons, Grebes, Ducks	Surf Scoter	*Melanitta perspicillata*	2.70	3.10	7.9	904
42	Loons, Grebes, Ducks	Pacific Loon	*Gavia pacifica*	0.60	0.70	8.3	1,301
43	Loons, Grebes, Ducks	Common Loon *	*Gavia immer*	0.10	0.10	8.2	562
44	Loons, Grebes, Ducks	Red-throated Loon	*Gavia stellata*	0.10	0.10	8.3	400